

RESEARCH MEMORANDUM

WIND-TUNNEL INVESTIGATION OF A RAM-JET MISSILE MODEL
HAVING A WING AND CANARD SURFACES OF DELTA
PLAN FORM WITH 70° SWEPT LEADING EDGES

FORCE AND MOMENT CHARACTERISTICS OF VARIOUS
COMBINATIONS OF COMPONENTS AT
A MACH NUMBER OF 1.6

By Clyde V. Hamilton, Cornelius Driver,
and John R. Sevier, Jr.

Langley Aeronautical Laboratory
Langley Field, Va.

**NATIONAL ADVISORY COMMITTEE
FOR AERONAUTICS
WASHINGTON**

March 9, 1953
Declassified January 20, 1958

NATIONAL ADVISORY COMMITTEE FOR AERONAUTICS

RESEARCH MEMORANDUM

WIND-TUNNEL INVESTIGATION OF A RAM-JET MISSILE MODEL
HAVING A WING AND CANARD SURFACES OF DELTA
PLAN FORM WITH 70° SWEEP LEADING EDGESFORCE AND MOMENT CHARACTERISTICS OF VARIOUS
COMBINATIONS OF COMPONENTS AT
A MACH NUMBER OF 1.6By Clyde V. Hamilton, Cornelius Driver,
and John R. Sevier, Jr.

SUMMARY

A ram-jet canard missile model having a wing and horizontal and vertical canard surfaces of delta plan form with 70° swept leading edges was tested in the Langley 4- by 4-foot supersonic pressure tunnel. Two ram-jet nacelles were mounted in the vertical plane on unswept pylons near the rear of the body. The center of gravity of the model was at -19.5 percent of the wing mean aerodynamic chord. Force characteristics of the missile configuration and various combinations of its components were determined at a Mach number of 1.61 and a Reynolds number of 3.83×10^6 based on the wing mean aerodynamic chord.

The slopes of the lift and moment curves for the body, body-wing, and body-wing-canard configurations agreed well with linear theory. All configurations with the wing on were longitudinally stable. The addition of nacelles to the body alone increased the longitudinal stability, but in the presence of the wing the nacelles produced a destabilizing moment.

An analysis of the drag breakdown indicated no significant drag interference effects. With the flow at the inlet choked (the only condition tested) the drag of the nacelle-pylon combination comprised 60 percent of the total drag of the complete configuration. Of this nacelle-pylon drag, approximately 36 percent was due to internal drag. A maximum lift-drag ratio of 3 was obtained for the complete configuration at an angle of attack of 10°.

Changes in nacelle position had little effect on the lift and drag of the complete model; however, as would be expected, the directional stability was increased by an outboard or rearward movement of the nacelle-pylon combination. The complete model had negative effective dihedral resulting from the roll increment produced by the nacelles.

INTRODUCTION

Tests have been made in the Langley 4- by 4-foot supersonic pressure tunnel to determine the aerodynamic characteristics of a ram-jet canard missile configuration at a Mach number of 1.61. The model had a wing and horizontal and vertical canard surfaces of delta plan form with 70° swept leading edges. Two ram-jet nacelles were mounted in the vertical plane on short unswept pylons near the rear of the body. The model was equipped with all-movable canard surfaces for both pitch and yaw control and movable wing-tip ailerons for roll control. The various component parts of the model could be removed to permit the investigation of the complete configuration or various combinations of its component parts to determine general interference effects.

The present investigation was part of a coordinated research program with the Langley Pilotless Aircraft Research Division. The object of the wind-tunnel program was to provide preflight aerodynamic data and to evaluate various interference effects not capable of determination in flight.

The results of the investigation of the stability and control characteristics of the complete model are presented in reference 1. This paper presents the longitudinal- and lateral-force characteristics of various combinations of the component parts of the model with the nacelle-pylon combination located in various positions. The reference center of gravity was at -19.5 per cent of the wing mean aerodynamic chord. Tests were run at a Mach number of 1.61 and a Reynolds number of 3.83×10^6 based on the wing mean aerodynamic chord.

COEFFICIENTS AND SYMBOLS

The results of the tests are presented as standard NACA coefficients of forces and moments. The data are referred to the stability-axes system (fig. 1) with the reference center of gravity at -19.5 percent of the wing mean aerodynamic chord.

The coefficients and symbols are defined as follows:

- C_L lift coefficient, $Lift/qS$, where $Lift = -Z$
- C_{L_F} lift-coefficient based on body frontal area, $Lift/qF$
- C_D drag coefficient, $Drag/qS$, where $Drag = -X$
- C_{D_F} drag coefficient based on body frontal area, $Drag/qF$

C_m	pitching-moment coefficient, $M'/qS\bar{c}$
C_{mF}	pitching-moment coefficient based on body length and body frontal area, M'/qFl
C_y	lateral-force coefficient, Y/qS
C_n	yawing-moment coefficient, N/qSb
C_l	rolling-moment coefficient L/qSb
Y	force along Y-axis, lb
Z	force along Z-axis, lb
M'	moment about Y-axis, lb-ft
L	moment about X-axis, lb-ft
N	moment about Z-axis, lb-ft
q	free-stream dynamic pressure, lb/sq ft
M	Mach number
S	total wing area, including body intercept, 0.6948 sq ft
S_H	horizontal canard area (exposed), 0.0222 sq ft
S_V	vertical canard area (exposed), 0.0222 and 0.0111 sq ft
F	body frontal area, 0.03875 sq ft
b	wing span, 0.988 ft
c	wing-section chord, ft
\bar{c}	wing mean aerodynamic chord, 0.957 ft, $\frac{2}{S} \int_0^{\frac{b}{2}} c^2 dy$
y	distance along wing span from model center line measured normal to plane of symmetry
l	body length, 4.23 ft
α	angle of attack of body center line, deg

β	angle of sideslip, deg
$C_{l\beta}$	effective-dihedral parameter, rate of change of rolling-moment coefficient with angle of sideslip per degree, $\partial C_l / \partial \beta$
$C_{m\alpha}$	rate of change of pitching-moment coefficient with angle of attack per degree, $\partial C_m / \partial \alpha$
L/D	ratio of lift to drag, C_L / C_D

Notation for configurations:

B	body
W	wing
N	nacelles and supporting pylons
H	horizontal canard surfaces
V	small vertical canard surfaces
V_L	large vertical canard surfaces

MODEL AND APPARATUS

A three-view drawing of the basic model is shown in figure 2 and of the canard control surfaces in figure 3. The various nacelle positions are shown in figure 4. A drawing of the wing showing the area considered enclosed within the body is shown in figure 5. The geometric characteristics of the model are given in table I.

The model was composed of a cylindrical body with a nose formed by a parabolic section and a frustum of a cone. Coordinates for the body are given in table II. The canard surfaces, figure 3, were in both the horizontal and vertical planes and had delta plan forms with 70° swept leading edges. The canard surfaces were all-movable and were deflected about an axis normal to the body center line. The vertical canards were of two sizes, the large one having the same area as the horizontal canards, and the small one having one-half the area of the horizontal canards. The main wing was located in the horizontal plane and was also of delta plan form with a 70° swept leading edge. The nacelles were mounted on short, unswept pylons. Coordinates for the nacelle and nacelle center body are given in table III. All components of the model were removable so that tests of various combinations of components could be made.

Force measurements were made through the use of a six-component internal strain-gage balance. The model was mounted in the tunnel on a 6° bent sting (ref. 1) to permit testing the model in combined pitch and yaw attitudes. By use of the bent sting, it was possible to test through the angle-of-attack range at sideslip angles of 0° and 6° and through the angle-of-sideslip range at angles of attack of 0° and 6°.

In order to determine the internal characteristics of the nacelle, a pressure survey rake with both total-pressure and static-pressure orifices was installed at the nacelle-exit plane for a portion of the test series.

The tests were conducted in the Langley 4- by 4-foot supersonic pressure tunnel. The tunnel is described in reference 2.

TESTS AND PROCEDURE

The test conditions were:

Mach number	1.61
Reynolds number, based on wing mean aerodynamic chord	3.83×10^6
Stagnation pressure, atm	1.0
Stagnation temperature, °F	110
Dew point, °F	< -25

The model configurations tested are listed in the following tables:

For the pitch tests -

α , deg	β , deg	Model configuration	Nacelle position
-4 to 14	0	B + W + N + H + V	Forward inboard
-4 to 12	0	B + W + N + H + V	Aft inboard
-4 to 14	0	B + W + N + H + V_L	Forward inboard
-4 to 12	0	B + W + N + H + V_L	Forward outboard
-4 to 10	0	B + W + N + H + V_L	Aft outboard
-4 to 10	0	B	-----
-4 to 3	0	B + W	-----
-4 to 10	0	B + H	-----
-4 to 10	0	B + H + V	-----
-4 to 12	0	B + N	Forward inboard
-4 to 14	0	B + W + N	Forward inboard
-4 to 4	0	B + W + H + V	-----
-4 to 8	0	B + N + H + V	Forward inboard
-4 to 12	0	B + W + H	-----

For the yaw tests -

α , deg	β , deg	Model configuration	Nacelle position
0	-3 to 8	B + W + H	-----
0 and 6	-4 to 10	B + W + N + H + V	Forward inboard
0	-4 to 10	B + W + N + H + V	Aft inboard
0	-4 to 10	B + W + N + H + V _L	Aft inboard
0	-4 to 10	B + W + N + H + L _L	Forward inboard
0	-4 to 10	B + W + N + H + V _L	Aft outboard
0	-4 to 12	B + W + N + H + V _L	Forward outboard
0	-4 to 10	B	-----
0 and 6	-4 to 10	B + W	-----
0	-4 to 10	B + H	-----
0	-4 to 8	B + V	-----
0	0 to 8	B + H + V	-----
0 and 6	-4 to 10	B + N	Forward inboard
0 and 6	-4 to 10	B + W + N	Forward inboard
0	-4 to 10	B + W + H + V	-----
0	-4 to 8	B + N + H + V	Forward inboard

CORRECTIONS AND ACCURACY

Results of a more complete calibration than that referred to in reference 1 indicate that the flow in the test section was reasonably uniform and that the Mach number was 1.61 instead of 1.60 in the area occupied by the model. The Mach number variation in the test section was ± 0.01 and the flow-angle variation in the horizontal and vertical planes was $\pm 0.1^\circ$. No corrections were applied to the data to account for these flow variations. The angles of attack and sideslip were corrected for the deflection of the balance under load. The base pressure was measured and the drag data were corrected to a base pressure equal to the free-stream static pressure. Errors in the base-pressure measurements are included in the estimated error of C_D . No corrections were made for sting interference.

The estimated errors in the individual measured quantities are as follows:

C_m	± 0.0004
C_L	± 0.004
C_D	± 0.0023
C_Y	± 0.001
C_n	± 0.0005
C_l	± 0.0004
α , deg	± 0.10
β , deg	± 0.10

RESULTS AND DISCUSSION

In most of the tests employing vertical canard surfaces, the small vertical canard surfaces were used; therefore, these will be the canard surfaces referred to unless otherwise designated. For these tests the complete basic model consists of the body, wing, twin nacelles with supporting pylons (forward inboard position), the horizontal canards, and the small vertical canards (B + W + N + H + V).

For all the tests the nacelles were open and the data include effects of internal flow. The nacelles were designed for a Mach number of approximately 2.10, but for this investigation the flow through the nacelles was subcritical and was choked near the lip. Because of the fixed geometry of the nacelle-center-body combination, the contraction ratio could not be reduced in order to permit starting.

Presentation of Results

A schlieren photograph showing the shock formation at the nacelle inlet is presented in figure 6. The aerodynamic characteristics in pitch of the complete model and various combinations of its components are presented in figures 7 to 11. Figure 12 presents the lift-drag ratios as a function of angle of attack for the complete model and various combinations of its components. Figure 13 presents the effects of nacelle position on the lift-drag ratios of the complete model. The aerodynamic characteristics in pitch of the body alone, body + wing, body + horizontal canard, and body + wing + horizontal canard and a comparison with theory are presented in figures 14 to 17. The aerodynamic characteristics in yaw of the complete model and various combinations of its components at $\alpha = 0^\circ$ and 6.3° are presented in figures 18 to 21.

Longitudinal Characteristics

Lift and pitch.- The complete basic model with the center of gravity at -19.5 percent of the mean aerodynamic chord is longitudinally stable (fig. 7) with a linear pitching-moment curve up to an angle of attack of approximately 11° at which point the slope of the pitching-moment curve $C_{m\alpha}$ becomes essentially zero up to $\alpha = 14.5^\circ$, which was the limit of the tests. All configurations with the wing on are longitudinally stable. The presence of the horizontal and vertical canard surfaces decreases the stability of the complete model. Figure 8 indicates that moving the nacelles inboard or moving the nacelle-pylon combination aft caused the presence of the nacelles to be less destabilizing. The nacelles in any position have a destabilizing effect on the complete model. The static margins for the various nacelle locations are:

Forward inboard nacelle	13.6 percent \bar{c}
Aft inboard nacelle	16.0 percent \bar{c}
Aft outboard nacelle	13.4 percent \bar{c}
Forward outboard nacelle.	10.7 percent \bar{c}

The static margin decreased with a forward or outboard shift in nacelle position.

The addition of the nacelles to the body alone (fig. 9) increased the total lift slightly and provided a small stabilizing moment to the body in direct opposition to the results for the complete model.

Drag.- A large portion of the drag at $\alpha = 0^\circ$ is due to the presence of the nacelles. The drag of the nacelles and supporting pylons (fig. 9) is about three times the drag of the body alone and approximately 60 percent of the drag of the complete configuration. The internal drag (fig. 8), as determined from a consideration of a momentum balance from free-stream conditions ahead of the inlet to conditions at the exit, indicates a value of internal drag which was approximately 36 percent of the measured nacelle-pylon drag.

The schlieren photograph (fig. 6) shows the shock formation at the nacelle inlet for the present investigation. (The nacelle design Mach number was 2.10.) The position of the conical shock and the fact that the normal shock was forward of the lip indicate that the additive drag and spillage losses were high in this off-design condition. The internal drag determined from a pressure survey of the exit was also very high. On the basis of an estimate of the nacelle drag (refs. 3 and 4) and the pylon drag, it is believed that the measured drag increment is approximately equal to the sum of the drags of the component parts; thus interference effects appear to be slight.

Slight changes in drag due to nacelle position are also evident (fig. 8). The forward inboard position has the smallest incremental drag of the four positions. Moving the nacelles outward increases the drag, chiefly because of the increased strut area. Moving the nacelles rearward also appears to increase the drag, although this increment is within the accuracy of the data.

The results of reference 3 show the same general trends with nacelle position as are shown in this report; however, comparison is necessarily limited because of basic differences between configurations tested.

Effect of vertical canard size.- The large and small vertical canards (fig. 11) have no effect upon the complete model in pitch. The drag of the configuration with the small vertical canards is higher than that with the large vertical canards apparently because of the higher thickness ratio and altered section of the small canard.

Lift-drag ratio.- The greatest penalty in L/D occurs when the nacelles are added (fig. 12) since the nacelles provide the largest increments in drag and decrease the lift of the wing. As previously stated, the data of references 3 and 4 indicate that this decrease in L/D would be expected because of the addition of the nacelle-pylon combination. A maximum value of L/D of approximately 3 was obtained for the complete configuration at $\alpha = 10^\circ$. Nacelle position had little effect on L/D (fig. 13).

Comparison with Theory

A comparison of the characteristics in pitch of the body alone based on body length and body frontal area (fig. 14) with the theory of reference 5 indicates good agreement throughout most of the angle-of-attack range. It should be noted that, for the drag curves of the body alone, the dashed curve represents the theoretical variation of drag coefficient with angle of attack based on the experimental drag coefficient at $\alpha = 0^\circ$.

For the B + W, B + H, and B + W + H configurations, the methods of references 6 and 7 were employed to predict the slope of the lift and pitching-moment curves. These methods employ a modified slender-body theory which does not include viscous effects. The theory as indicated in figures 15 to 17 is, therefore, modified to include viscous effects on the body as determined from reference 5. For the case of the B + W + H configuration, the theory was determined by first calculating the slopes for the B + H configuration by the methods of references 6 and 7 and then adding the effect of the wing alone. The lift of the wing alone was determined from the data of reference 8 and the center of pressure was assumed to be at two-thirds of the root chord. This method, of course, does not consider the wing-body interference effects or any shift with angle of attack of the wing center of pressure. Downwash effects of the canard surfaces on the wing also were determined by the method of reference 9. Figure 10 indicates that the downwash effects of the canard surfaces on the wing decrease the lift of the wing by an amount approximately equal to the lift of the canard surfaces. These effects are in agreement with the theory advanced in reference 9. The agreement of theory with the experimental data is reasonably good.

Lateral Characteristics

Directional stability of the basic model.- In general, the model is directionally stable for configurations with the nacelle-pylon combination on and unstable with it off (fig. 18). The wings and horizontal canards have little effect on the directional stability of the complete model. The flagged symbols (fig. 18(b)) represent a check run on the

complete configuration. The discrepancies in yawing moment between the two runs are probably due to model or canard misalignment.

The body alone (fig. 19) is unstable directionally with the wings and horizontal canards having no effect on the directional stability. The nacelles (forward inboard position) provide the directional stabilizing moments as indicated previously.

Rolling moments of the basic model.- At an angle of attack of 0° (fig. 18(a)), rolling moments for all configurations are essentially zero since the model is symmetrical. The slight deviations from zero rolling moment are due to asymmetric conditions in the tunnel and to model misalignment. At an angle of attack of 6.3° (fig. 18(b)), the complete basic model has negative effective dihedral, or positive $C_{l\beta}$.

The body + wing configuration has a negative value of $C_{l\beta}$ or positive effective dihedral. The addition of the nacelles to the body-wing configuration results in a large positive value of $C_{l\beta}$. The addition of the horizontal and vertical canards or the wing shifts the value of $C_{l\beta}$ in a negative direction.

Effect of canard size.- The basic configuration (forward inboard nacelle position) with the large vertical canards (fig. 20), that is, vertical canards with the same area as the horizontal canards, is neutrally stable directionally in the region where $\beta = 0^\circ$ and is unstable throughout most of angle-of-sideslip range. When the area of the vertical canards is halved, as in the case of the small vertical canards, the complete model becomes stable directionally throughout the angle-of-sideslip range.

Effect of nacelle position.- Figure 21 indicates that, with the nacelles in the outboard position, which involves an increase in pylon area, the directional stability is increased. Moving the nacelles aft further increases directional stability because of the increased moment arm. An aft or an outboard shift of the nacelles, or both, would probably increase the positive value of $C_{l\beta}$.

CONCLUSIONS

A ram-jet canard missile model having a wing and horizontal and vertical canard surfaces of delta plan form with 70° swept leading edges was tested in the Langley 4- by 4-foot supersonic pressure tunnel. Two ram-jet nacelles were mounted in the vertical plane on unswept pylons near the rear of the body. The center of gravity of the model was at -19.5 percent of the mean aerodynamic chord. Force characteristics of

the missile configuration and various combinations of its components were determined at a Mach number of 1.61 and a Reynolds number of 3.83×10^6 , based on the wing mean aerodynamic chord. The results of this investigation indicated the following conclusions:

1. The slopes of the lift and moment curves for the body, body-wing, and body-wing-canard configurations agreed well with linear theory.

2. All configurations with the wing on were longitudinally stable. The addition of nacelles to the body alone increased the longitudinal stability, but in the presence of the wing the nacelles produced a destabilizing moment.

3. An analysis of the drag breakdown indicated no significant drag interference effects. With the flow at the inlet choked (the only condition tested) the drag of the nacelle-pylon combination comprised 60 percent of the total drag of the complete configuration. Of this nacelle-pylon drag, approximately 36 percent is due to internal drag. A maximum lift-drag ratio of 3 was obtained for the complete configuration at an angle of attack of 10° .

4. Changes in nacelle position had little effect on the lift and drag of the complete model; however, as would be expected, the directional stability was increased by an outboard or rearward movement of the nacelle-pylon combination.

5. The complete model had negative effective dihedral resulting from the roll increment produced by the nacelles.

Langley Aeronautical Laboratory,
National Advisory Committee for Aeronautics,
Langley Field, Va., January 6, 1953

REFERENCES

1. Spearman, M. Leroy, and Robinson, Ross B.: Wind-Tunnel Investigation of a Ram-Jet Canard Missile Model Having a Wing and Canard Surfaces of Delta Plan Form With 70° Swept Leading Edges. Longitudinal and Lateral Stability and Control Characteristics at a Mach Number of 1.60. NACA RM L52E15, 1952.
2. Spearman, M. Leroy, and Hilton, John H., Jr.: Aerodynamic Characteristics at Supersonic Speeds of a Series of Wing-Body Combinations Having Cambered Wings With an Aspect Ratio of 3.5 and a Taper Ratio of 0.2. Effects of Sweep Angle and Thickness Ratio on the Static Lateral Stability Characteristics at $M = 1.60$. NACA RM L51K15a, 1952.
3. Madden, Robert T., and Kremzier, Emil J.: Data Presentation of Force Characteristics of Several Engine-Strut-Body Configurations at Mach Numbers of 1.8 and 2.0. NACA RM E51E29, 1951.
4. Weinstein, Maynard I., and Davids, Joseph: Force and Pressure Characteristics for a Series of Nose Inlets at Mach Numbers From 1.59 to 1.99. III - Conical-Spike All-External-Compression Inlet With Supersonic Cowl Lip. NACA RM E50J30, 1951.
5. Allen, H. Julian: Estimation of the Forces and Moments Acting on Inclined Bodies of Revolution of High Fineness Ratio. NACA RM A9I26, 1949.
6. Nielsen, Jack N., and Kaattari, George E.: Method for Estimating Lift Interference of Wing-Body Combinations at Supersonic Speeds. NACA RM A51J04, 1951.
7. Kaattari, George E., Nielsen, Jack N., and Pitts, William C.: Method for Estimating Pitching-Moment Interference of Wing-Body Combinations at Supersonic Speed. NACA RM A52B06, 1952.
8. Ribner, Herbert S., and Malvestuto, Frank S., Jr.: Stability Derivatives of Triangular Wings at Supersonic Speeds. NACA Rep. 908, 1948. (Supersedes NACA TN 1572.)
9. Morikawa, George: Supersonic Wing-Body-Tail Interference. Jour. Aero. Sci., vol. 19, no. 5, May 1952, pp. 333-340.

TABLE I.- GEOMETRIC CHARACTERISTICS OF MODEL

Body:	
Maximum diameter, in.	2.666
Length, in.	50.833
Fineness ratio	19.067
Base area, sq in.	5.583
Wing:	
Span in.	11.853
Chord at body center line, in.	17.069
Chord at aileron break line, in.	4.606
Area (including that within body) sq in.	100.049
Aspect ratio	1.404
Sweep angle of leading edge, deg	70
Thickness ratio at body center line.	0.0147
Thickness ratio at aileron break line.	0.0543
Leading-edge angle normal to leading edge, deg	15.6
Mean aerodynamic chord, in.	11.48
Aileron:	
Area, sq in.	3.201
Mean aerodynamic chord, in.	3.071
Large canard surfaces:	
Area (exposed), sq in.	6.406
Mean aerodynamic chord, in.	2.576
Small vertical canard surfaces:	
Area (exposed), sq in.	3.203
Mean aerodynamic chord, in.	1.821

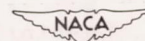


TABLE II.- BODY COORDINATES

Body station	Radius
0	0
.297	.076
.627	.156
.956	.233
1.285	.307
1.615	.378
1.945	.445
2.275	.509
2.605	.573
2.936	.627
3.267	.682
3.598	.732
3.929	.780
4.260	.824
4.592	.865
4.923	.903
5.255	.940
5.587	.968
5.920	.996
6.252	1.020
6.583	1.042
11.542	1.333
50.833	1.333

} conical section
 } cylindrical section

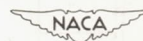
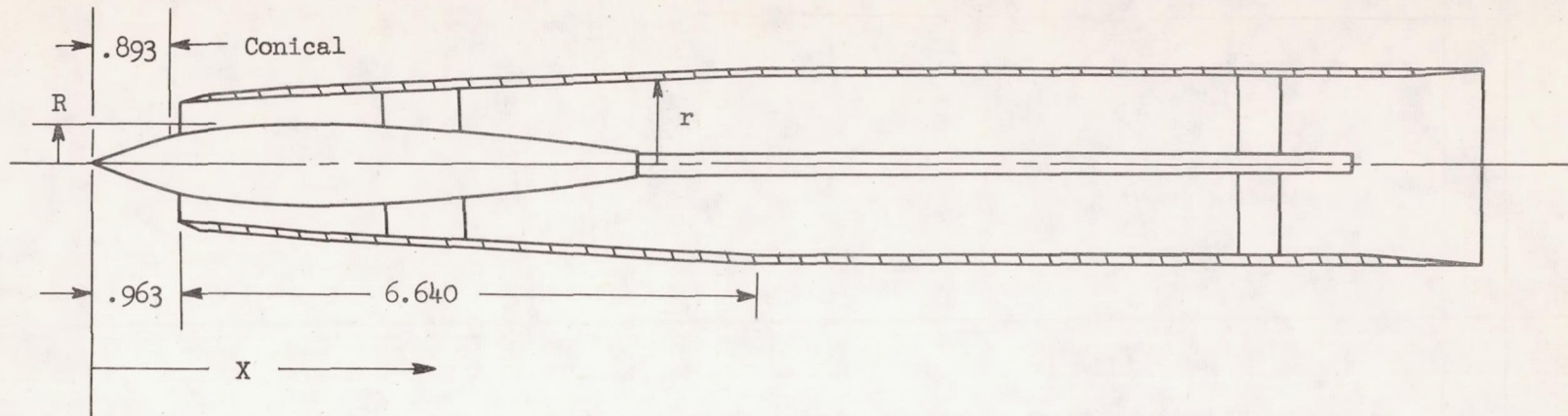
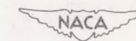

 NACA

TABLE III.- NACELLE AND NACELLE-CENTER-BODY GEOMETRY

NACA RM 153A14



X	R	X	r
0	0		
.893	.325	.963	^a .706
1.000	.360	7.603	^a .996
1.167	.402	13.712	^a .996
1.333	.429	14.962	^a 1.069
1.375	.433		
1.500	.441		
1.667	.443		
2.333	.418		
3.000	.375		
6.208	.157		



^aAll internal contours are straight surfaces between the points noted.

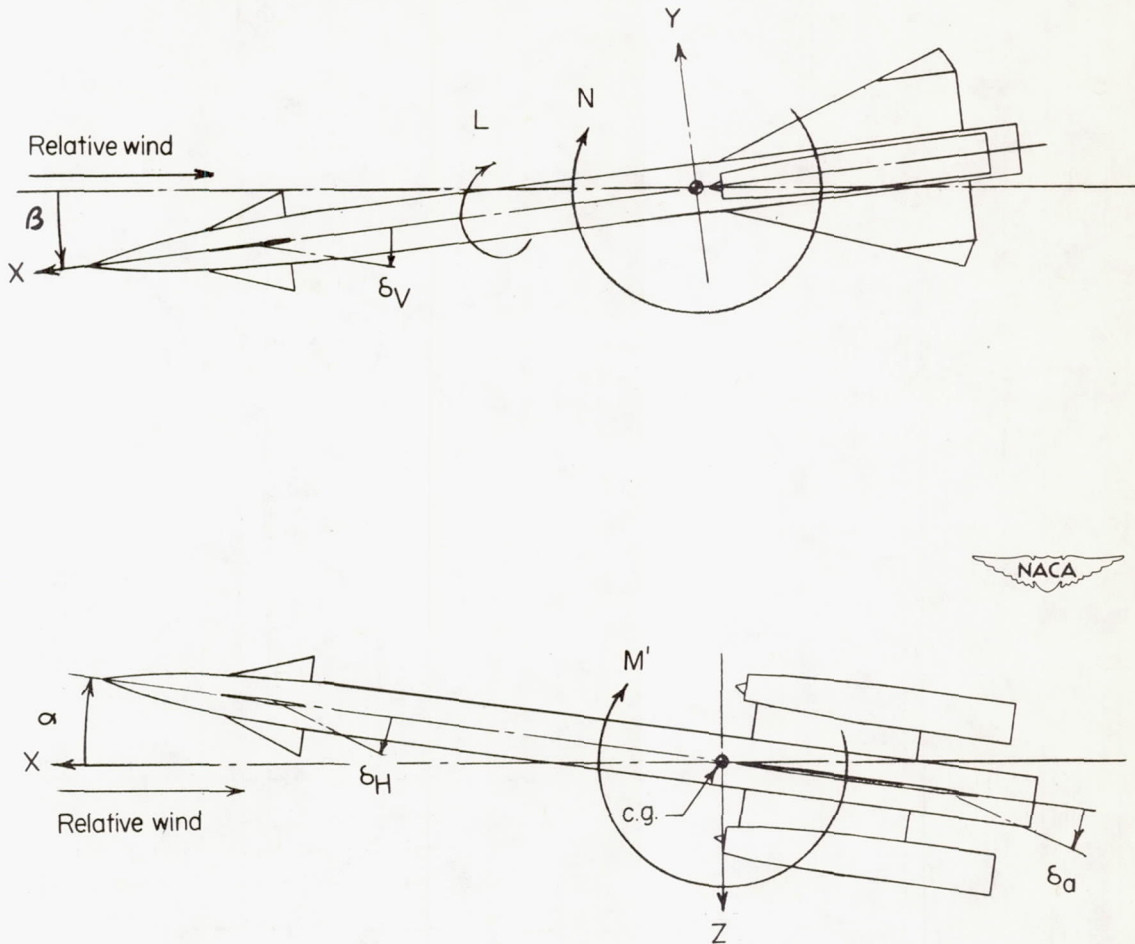


Figure 1.- System of stability axes. Arrows indicate positive values.

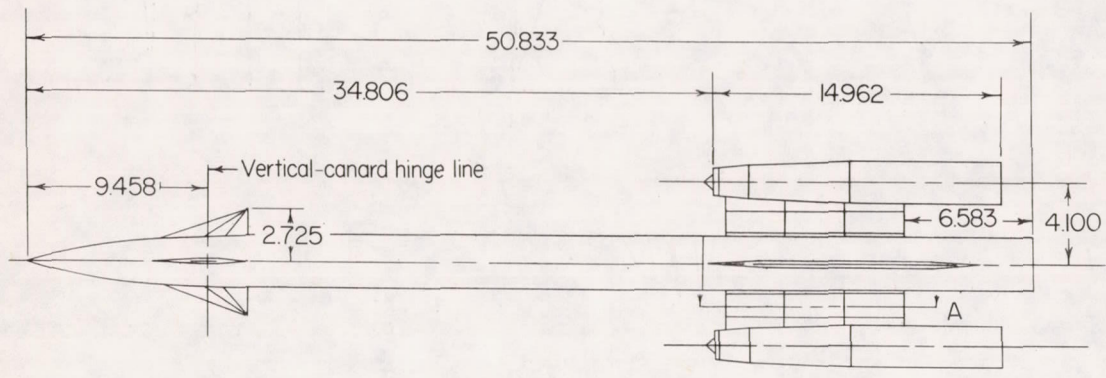
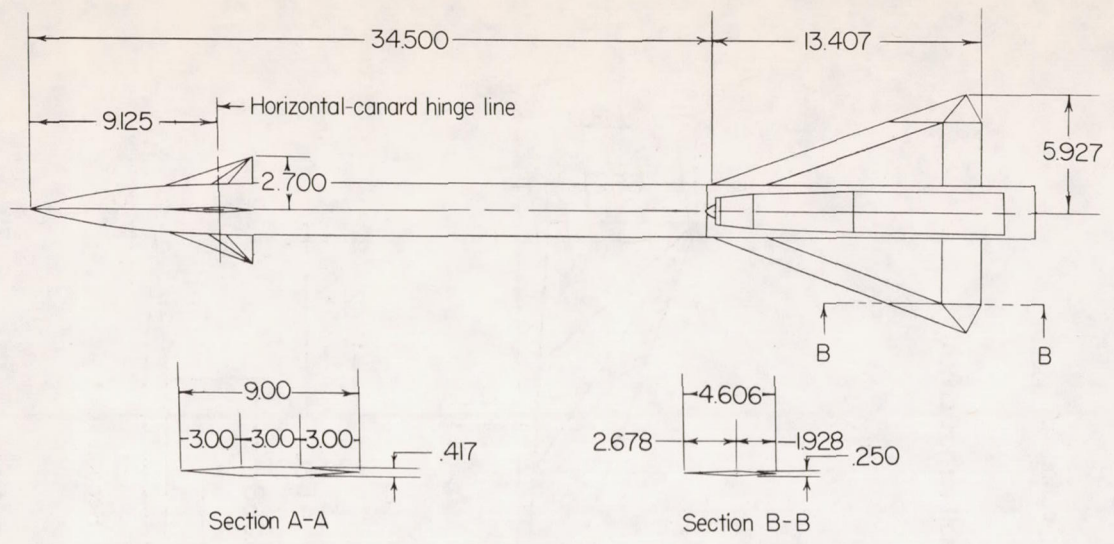
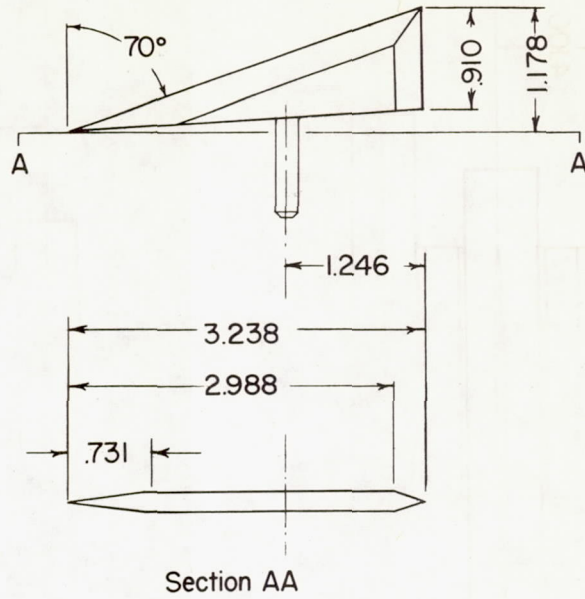
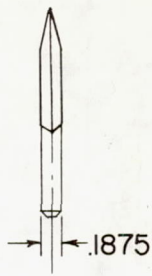
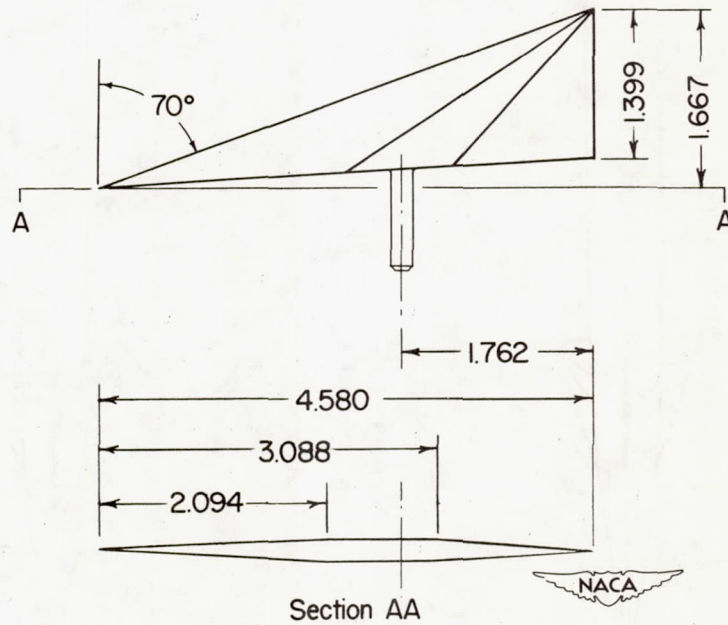
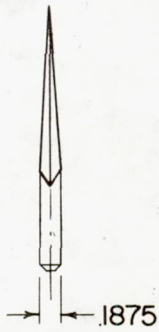


Figure 2.- Details of ram-jet canard missile model. All dimensions in inches.



Small vertical canard



Large vertical and horizontal canard

Figure 3.- Control-surface details. All dimensions in inches.

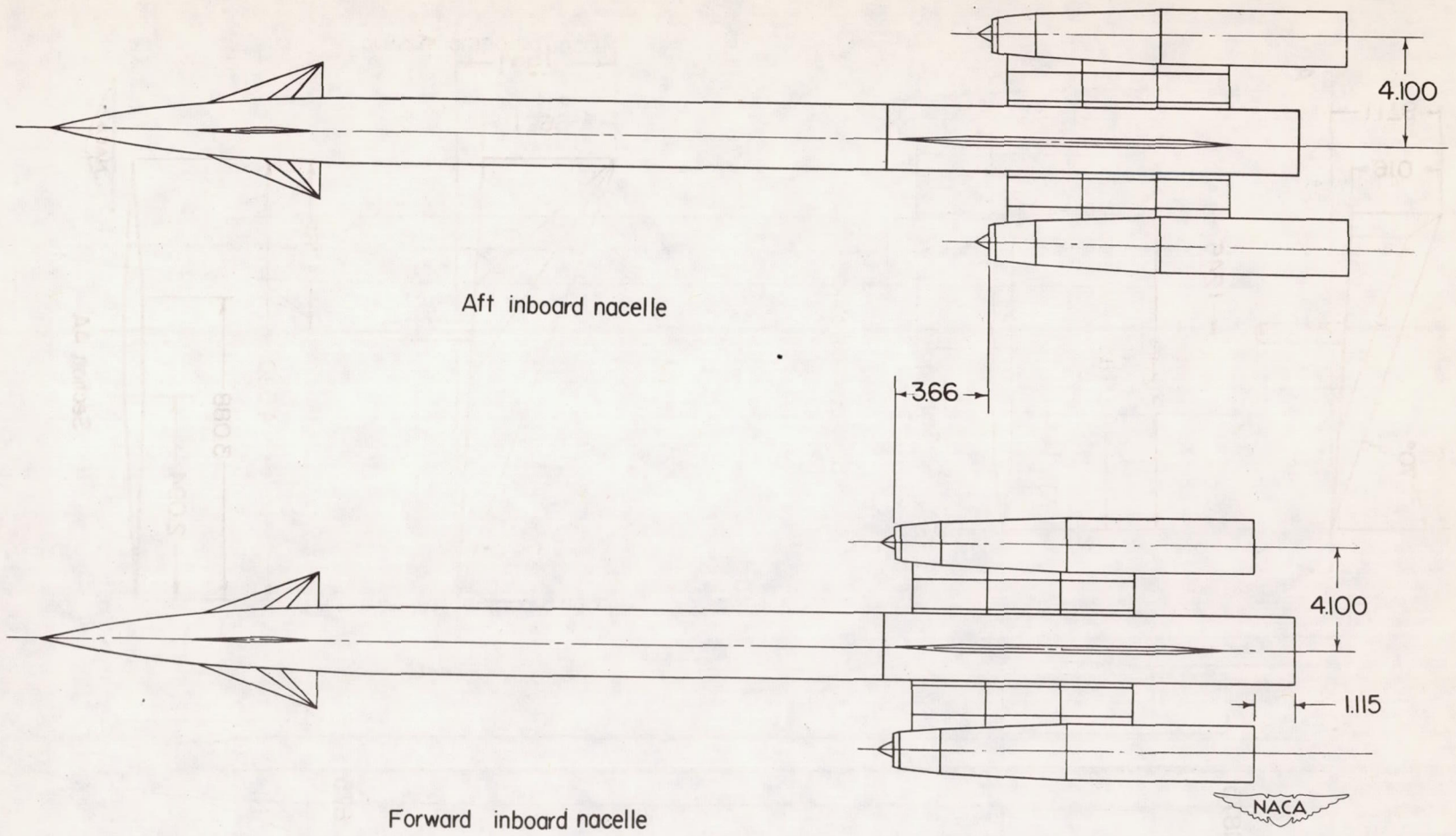


Figure 4.- Sketches of four nacelle positions investigated.

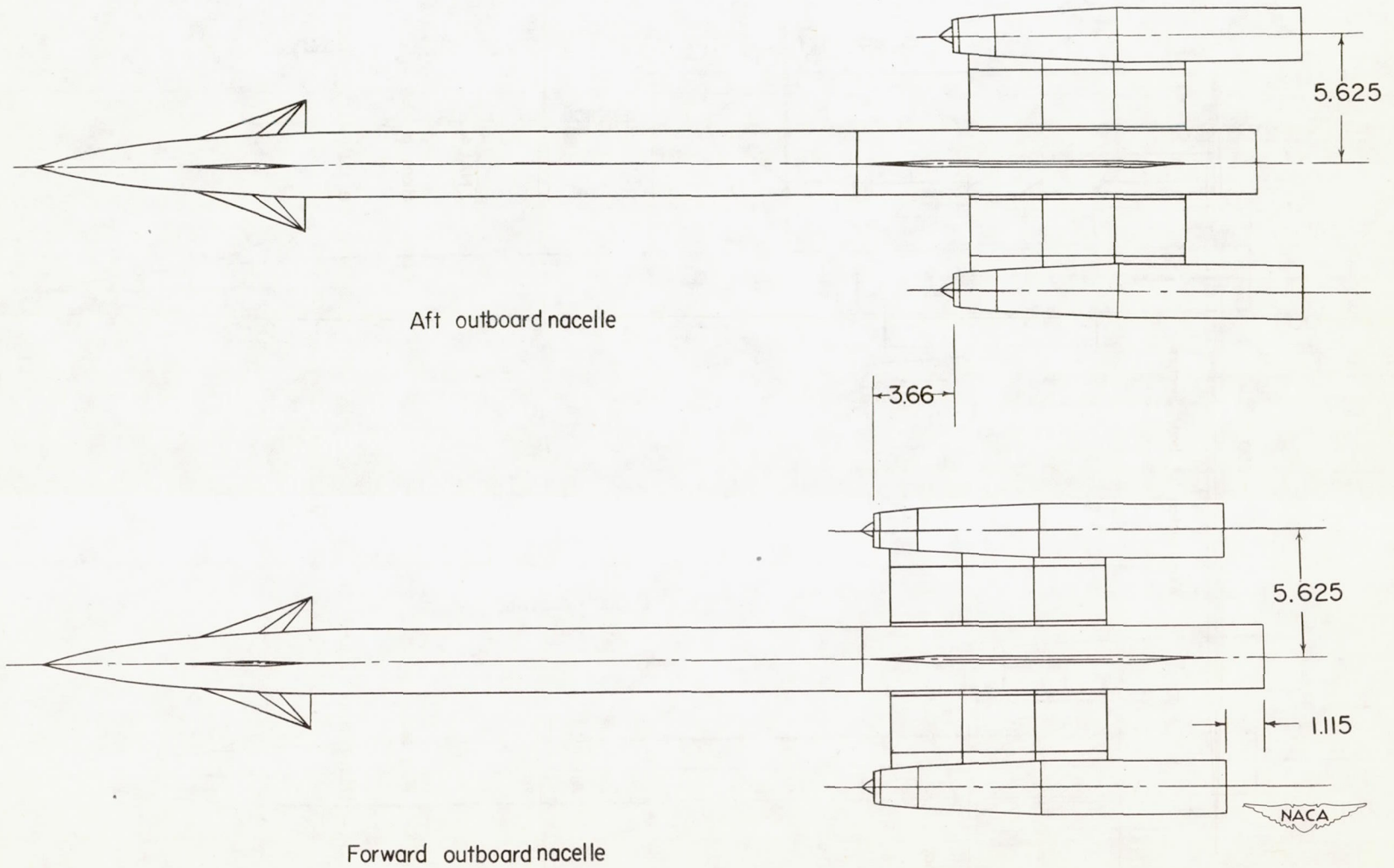


Figure 4.- Concluded.

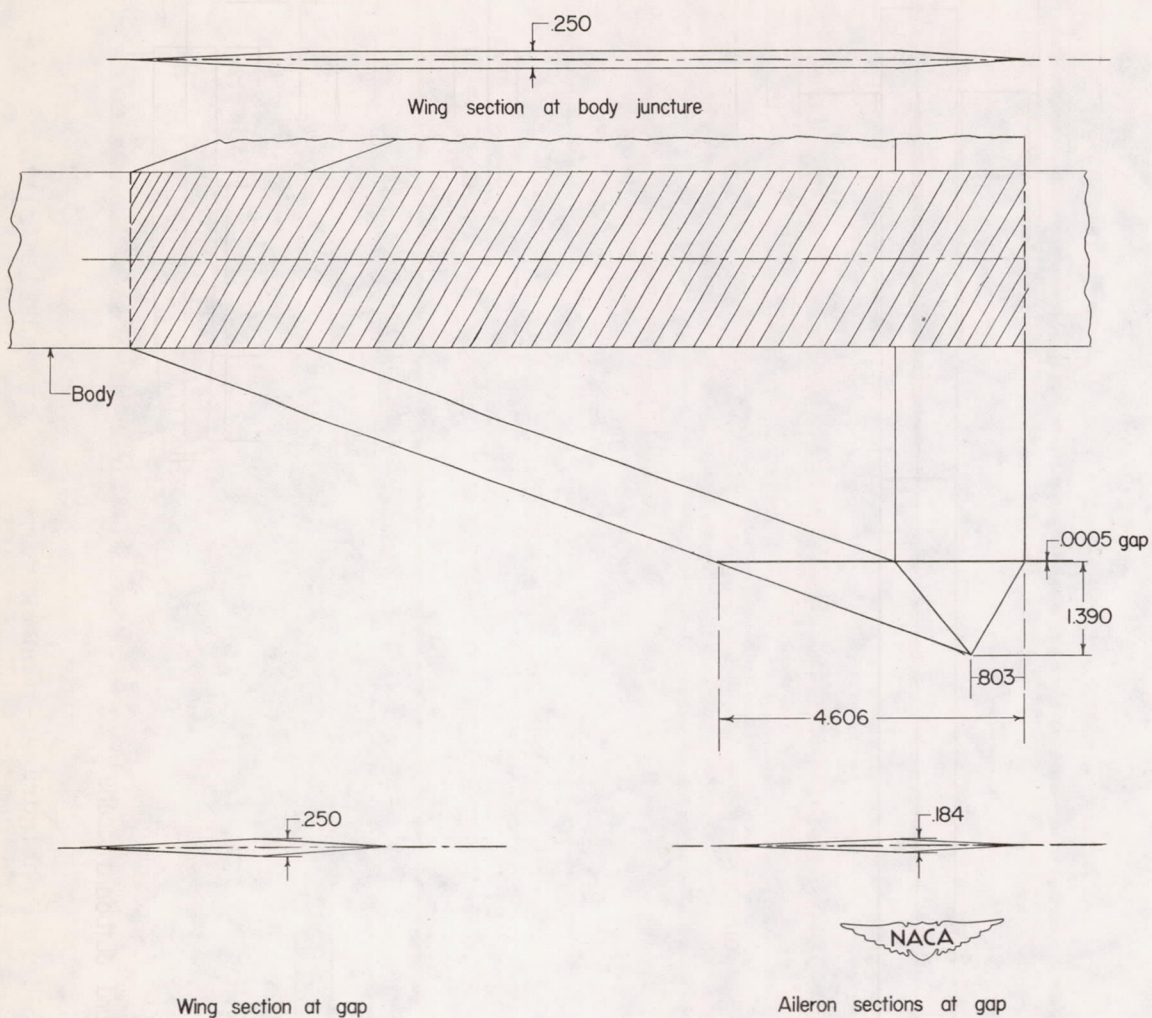


Figure 5.- Wing and aileron. Shaded area indicates area of wing enclosed by body. All dimensions in inches.

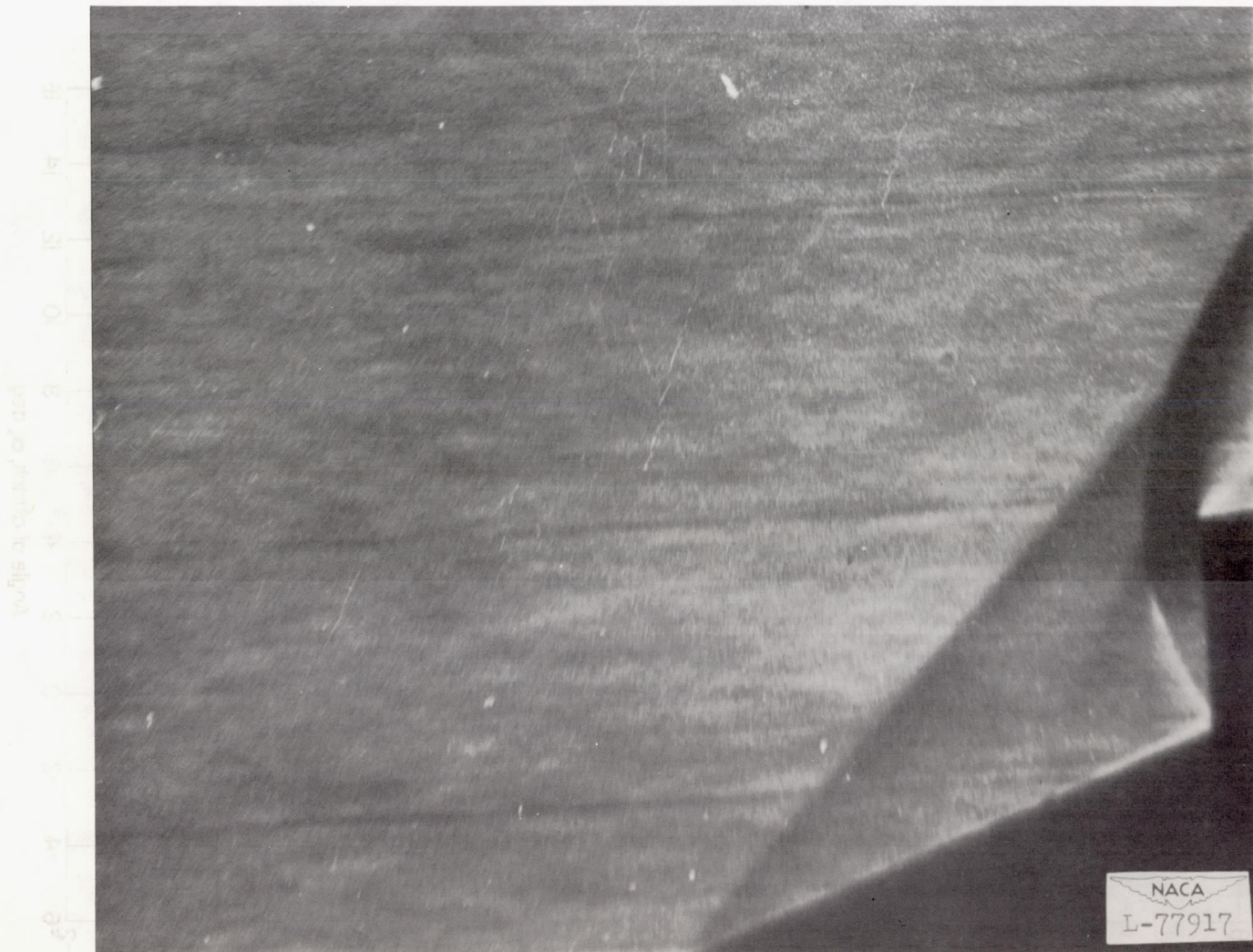


Figure 6.- Schlieren photograph of shock formation at nacelle inlet.
 $\alpha = 0^\circ$; $\beta = 0^\circ$; $M = 1.61$.

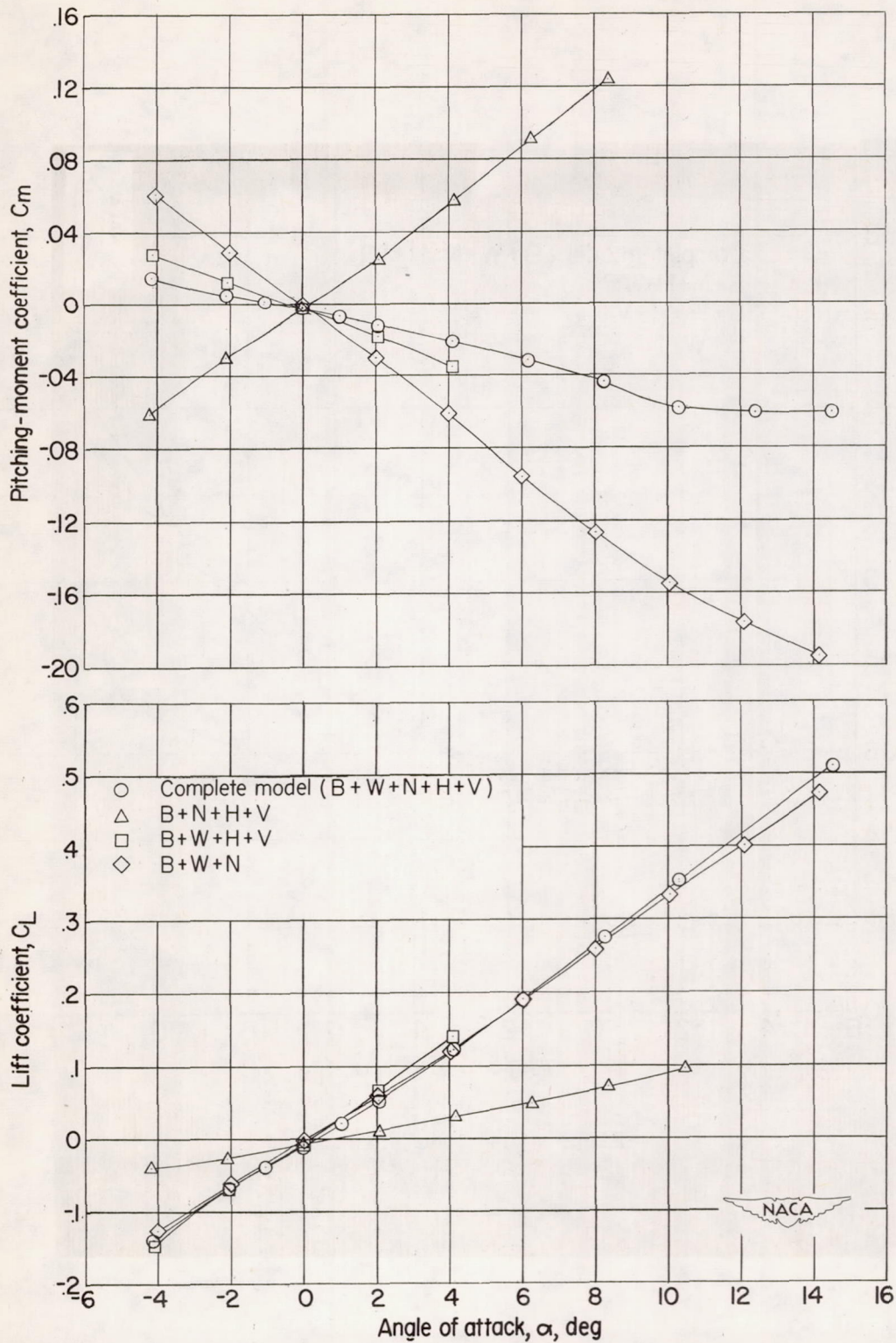


Figure 7.- Effect of various components on the aerodynamic characteristics in pitch of the complete basic model. $M = 1.61$.

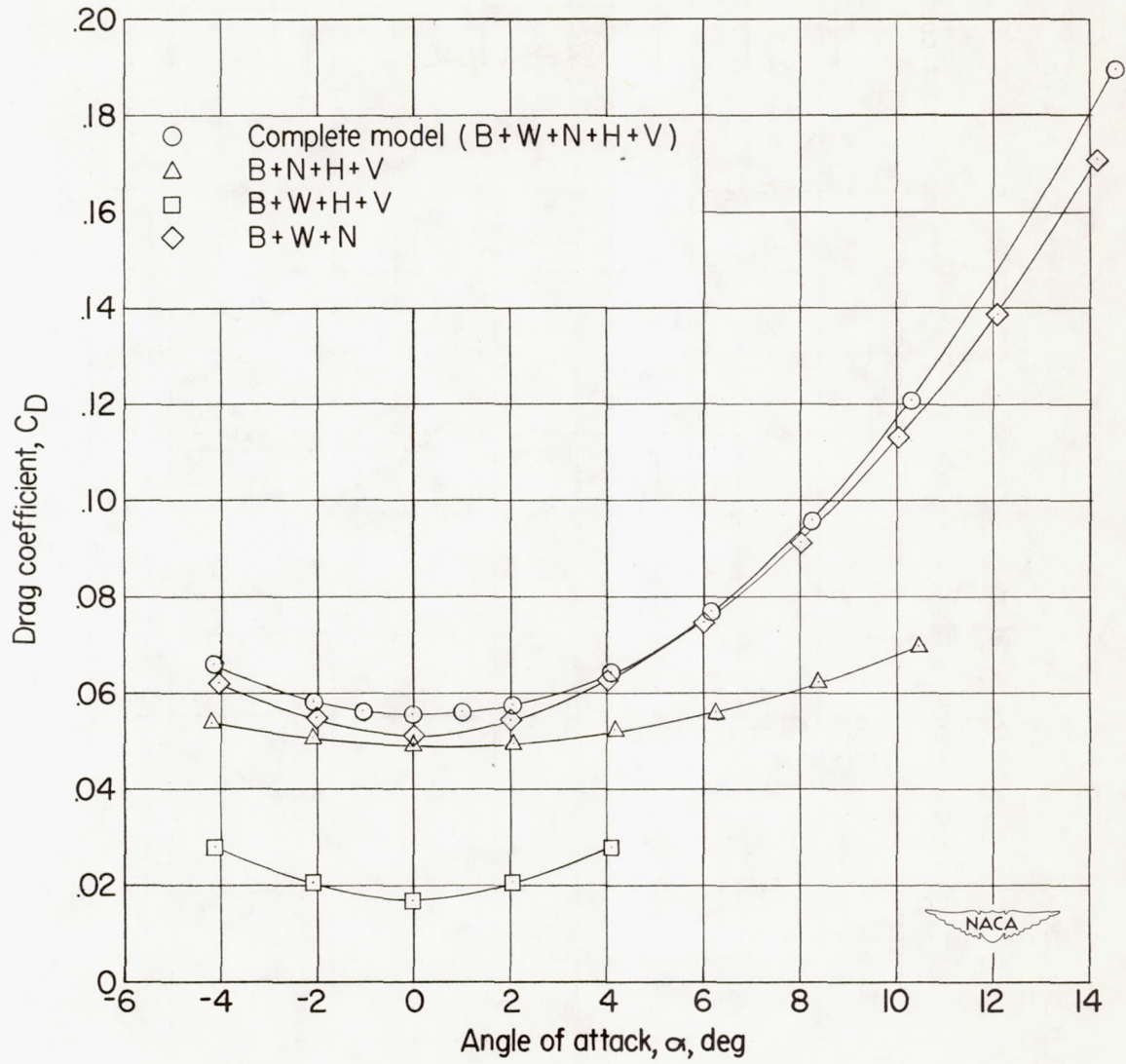


Figure 7.- Concluded.

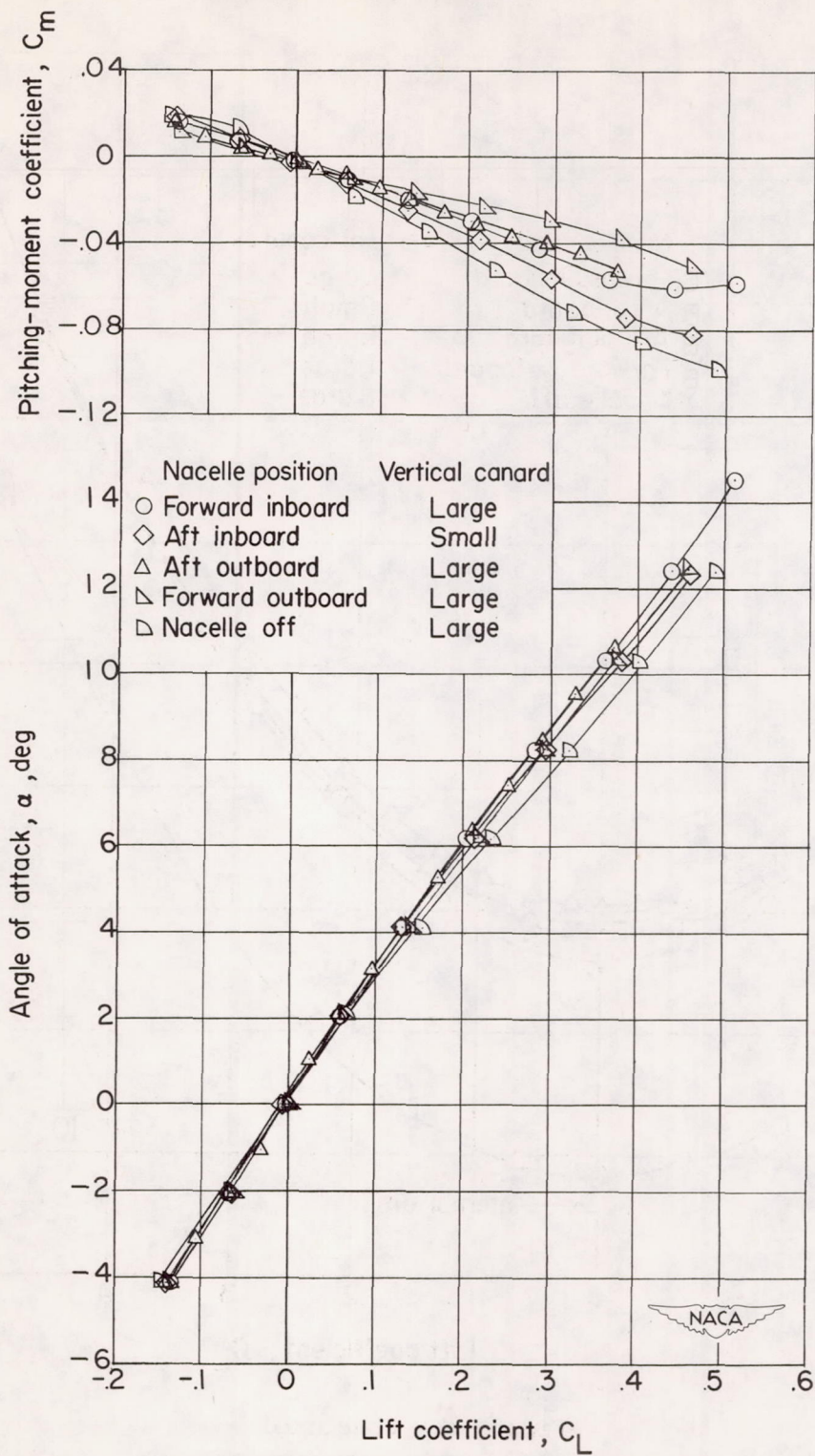


Figure 8.- Effect of nacelle position on the aerodynamic characteristics in pitch. $M = 1.61$.

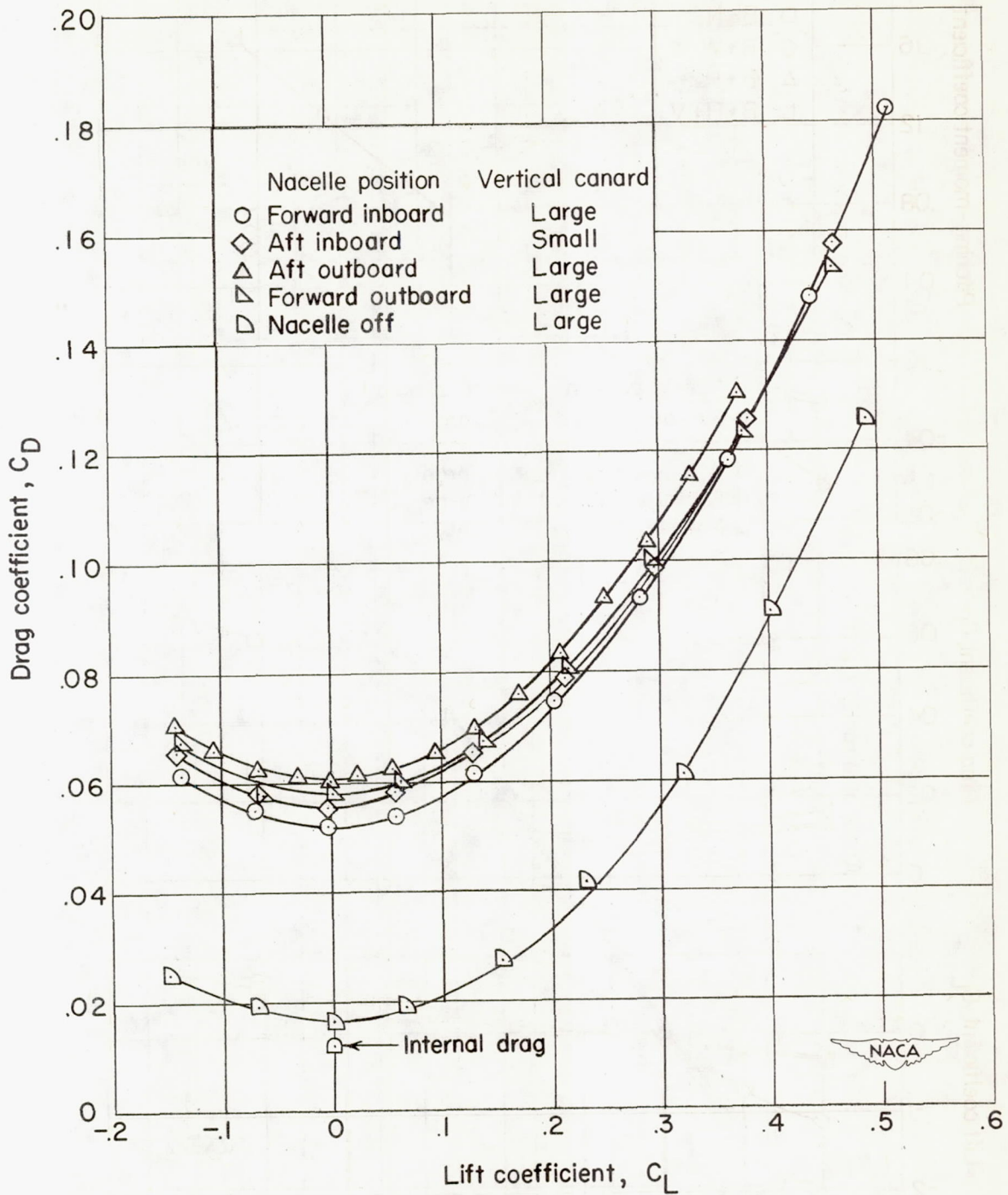


Figure 8.- Concluded.

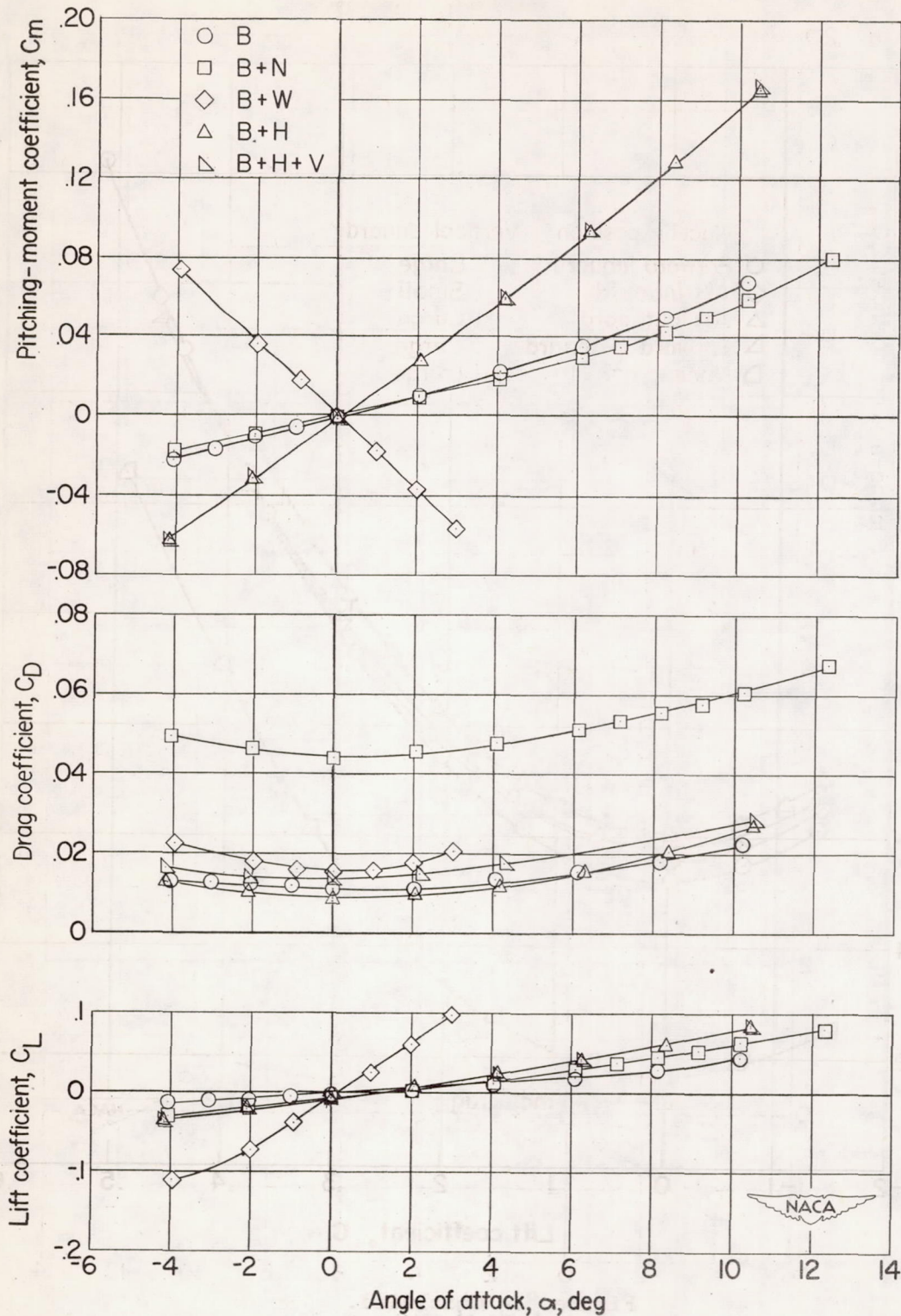


Figure 9.- Effect of various components on the aerodynamic characteristics in pitch of the body alone. $M = 1.61$.

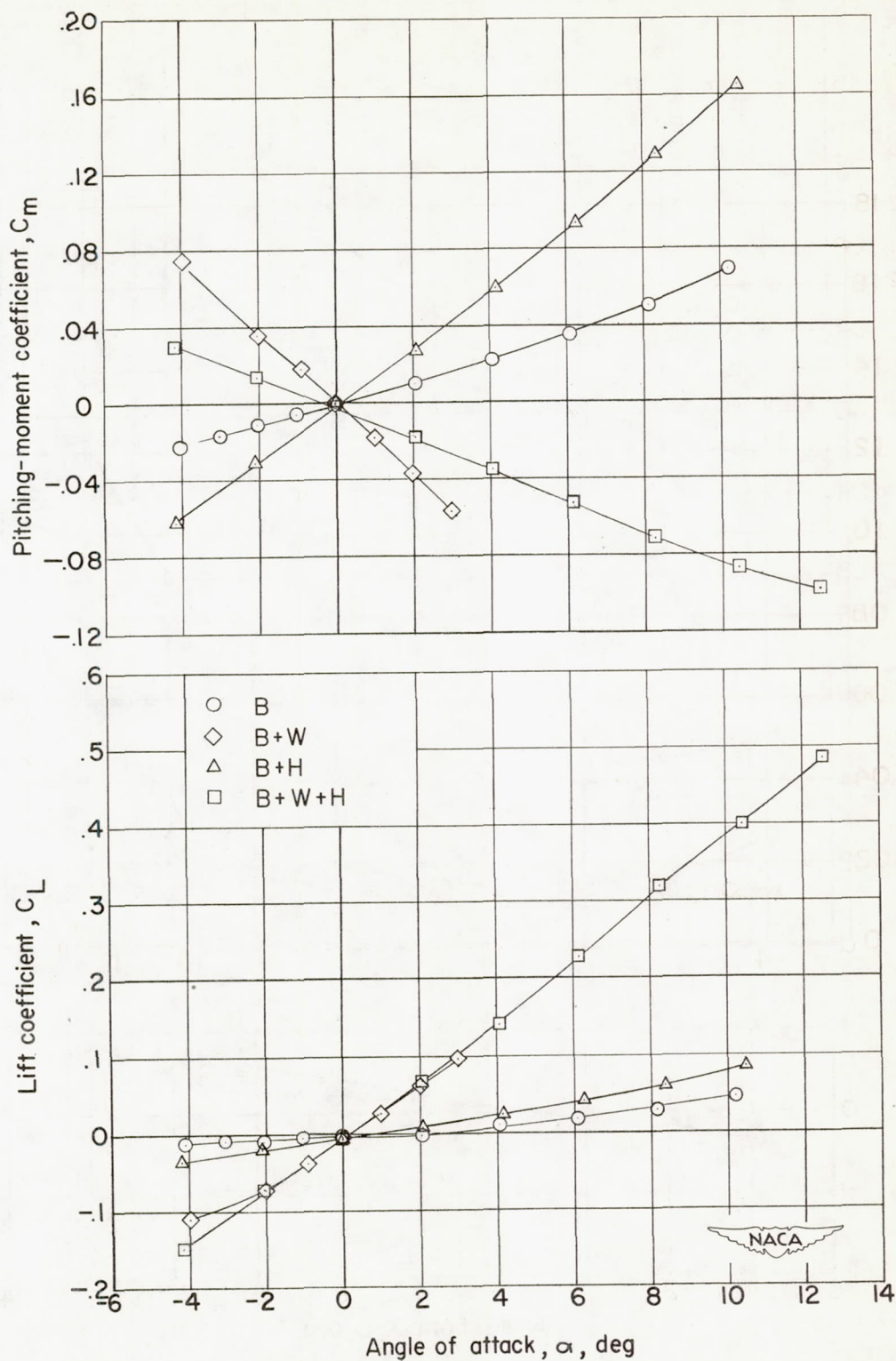


Figure 10.- Effect of horizontal canards on the aerodynamic characteristics in pitch of a body-wing combination. $M = 1.61$.

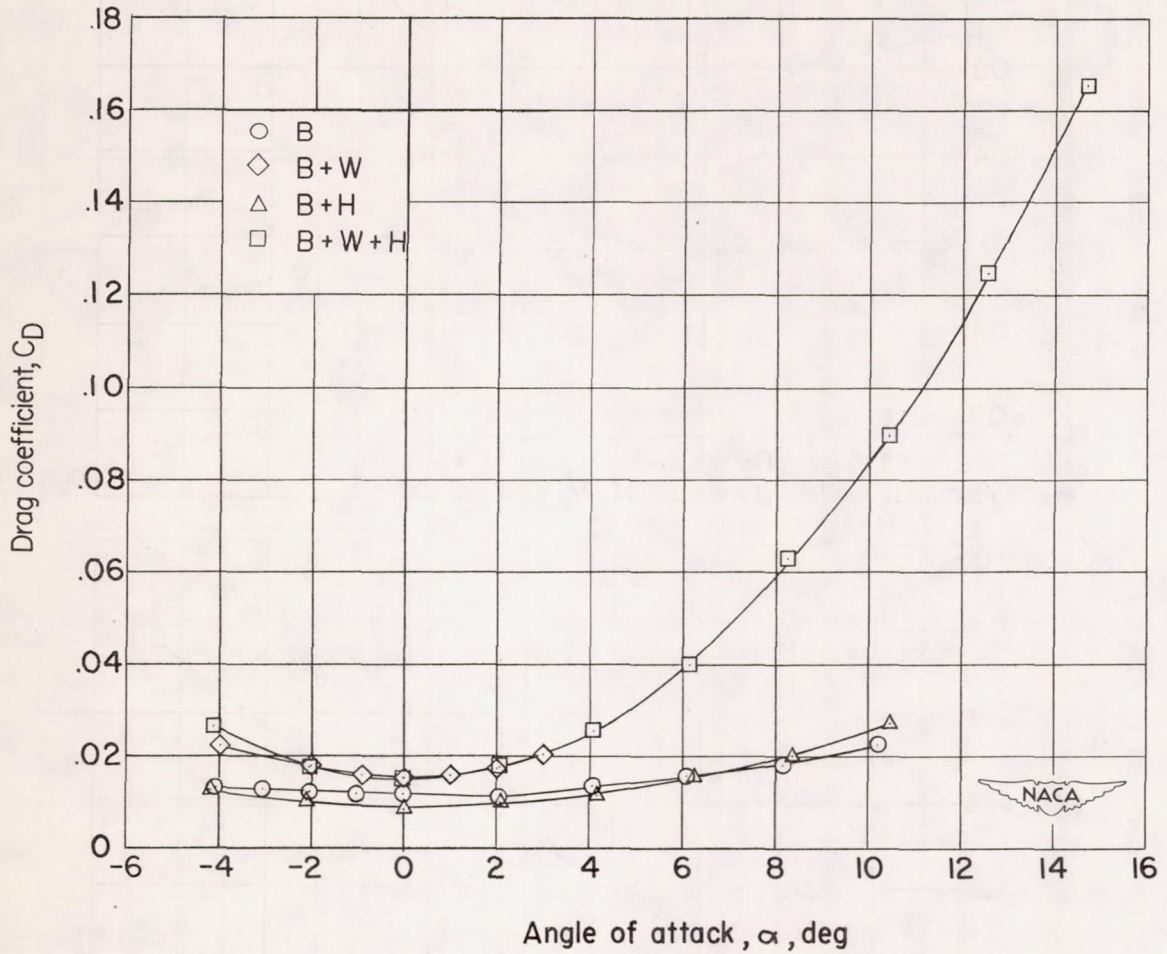


Figure 10.- Concluded.

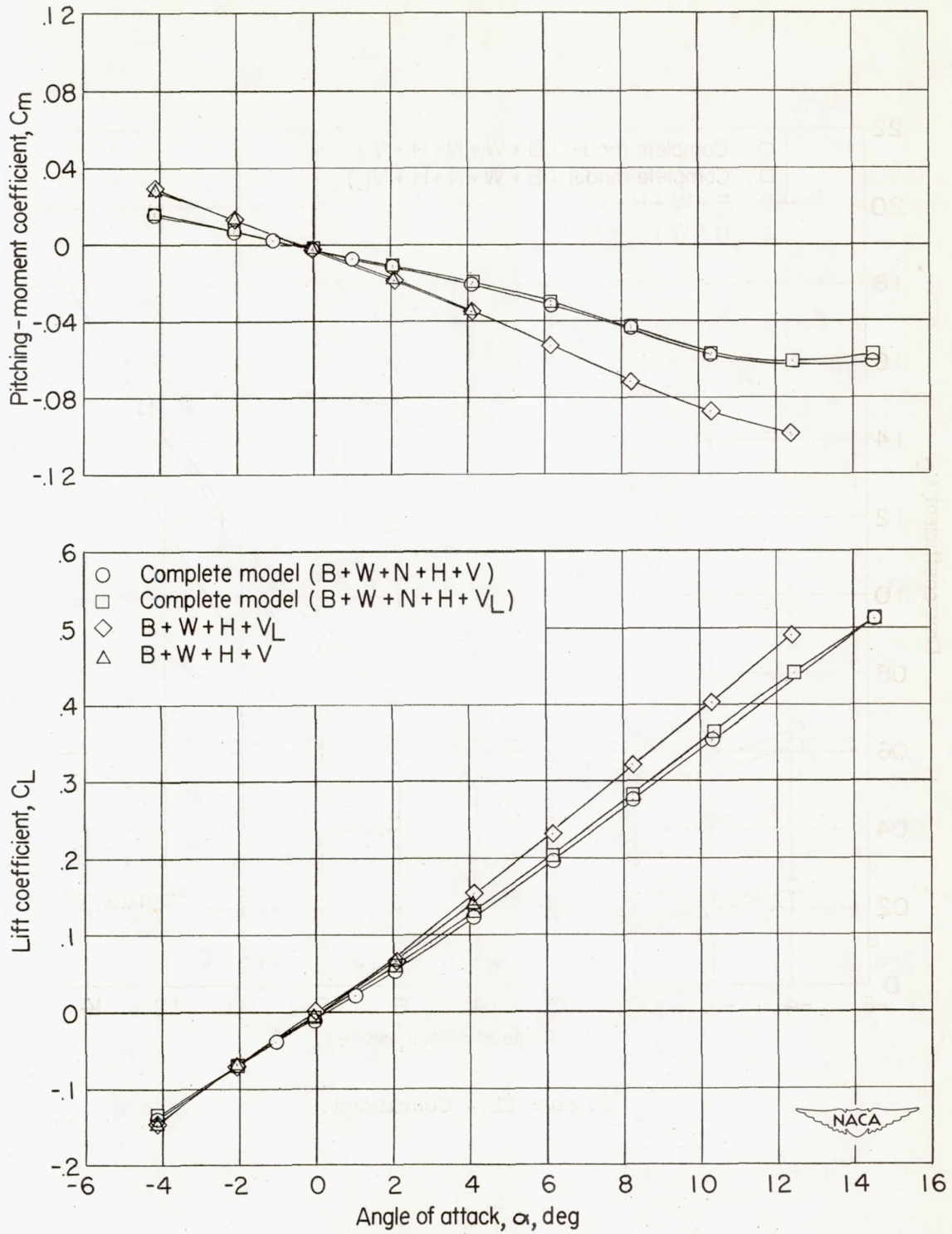


Figure 11.- Effect of vertical canard size on the aerodynamic characteristics in pitch of the complete basic model. $M = 1.61$.

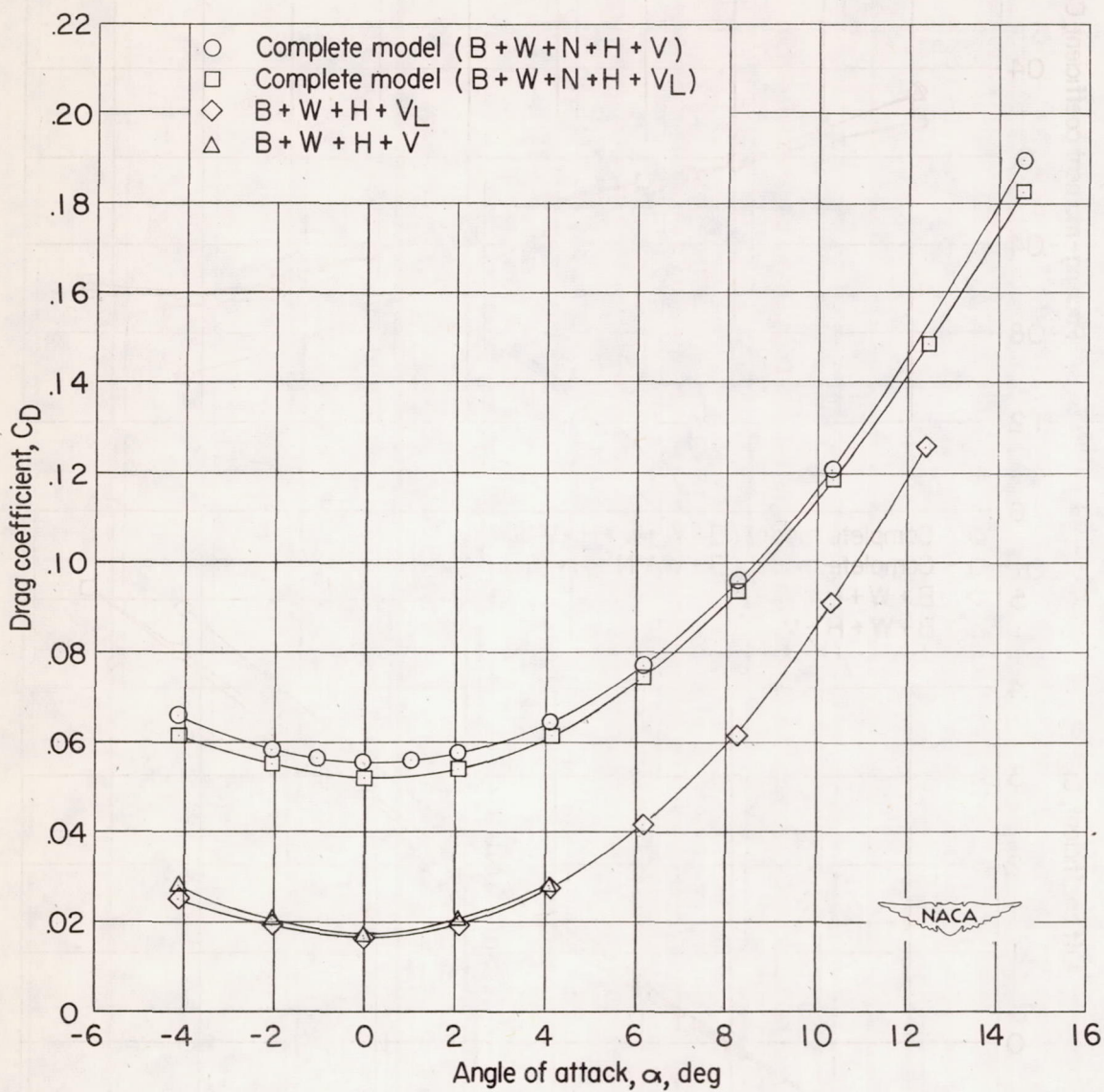


Figure 11.- Concluded.

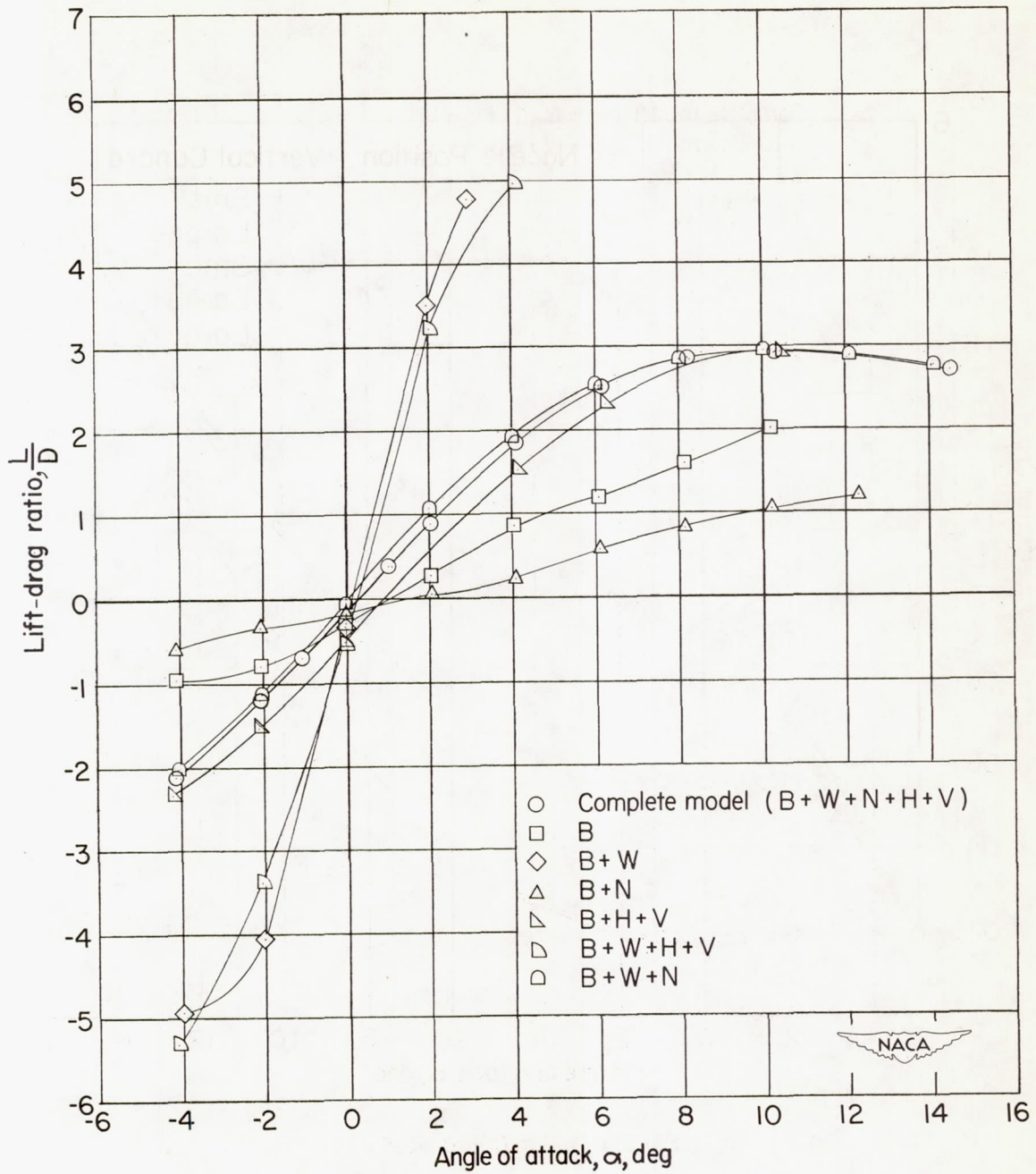


Figure 12.- Lift-drag ratio L/D as a function of angle of attack for the complete basic model and various combinations of its components. $M = 1.61$.

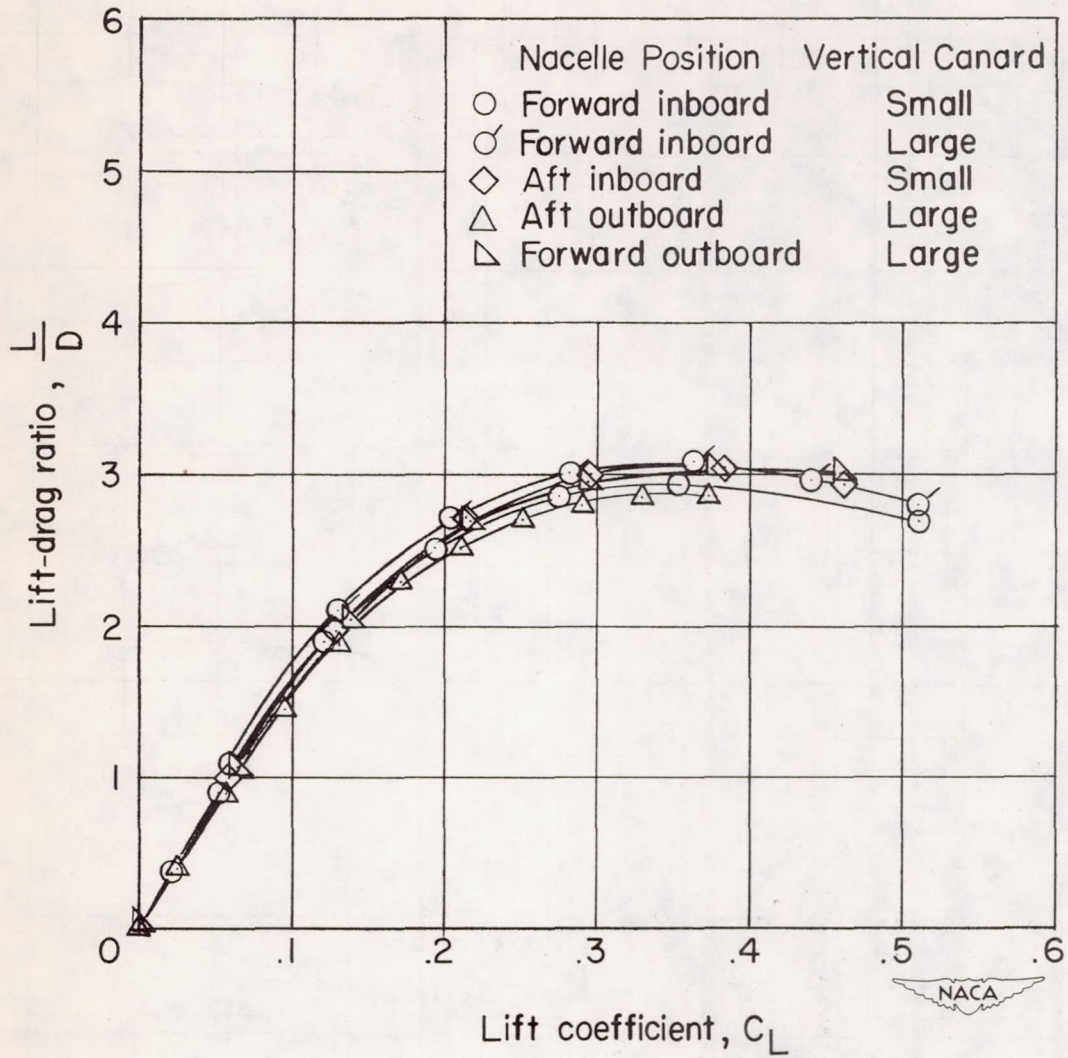


Figure 13.-- Effect of nacelle position on the lift-drag ratio for the complete model. $M = 1.61$.

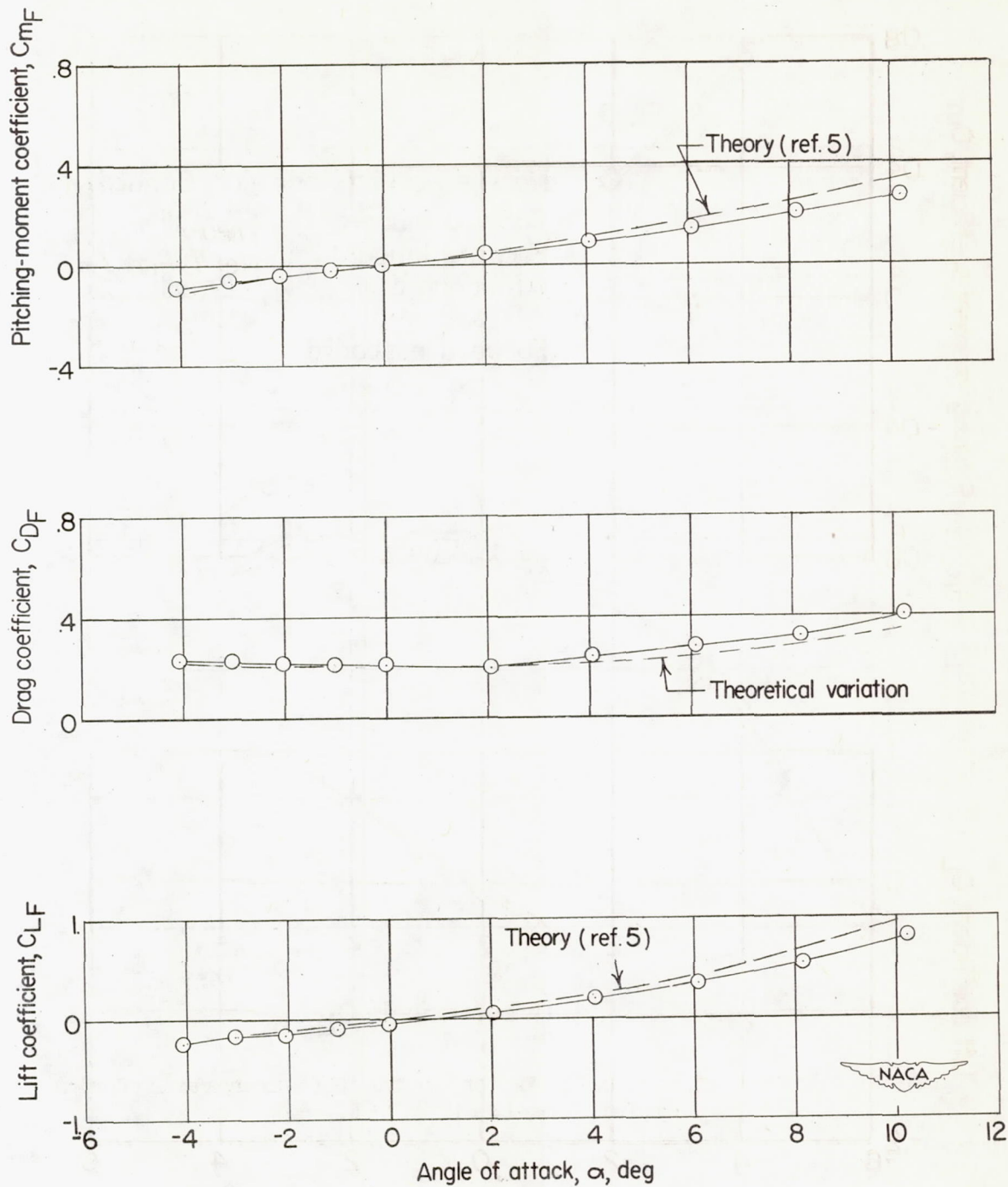


Figure 14.- Aerodynamic characteristics in pitch of the body alone.
 $M = 1.61$.

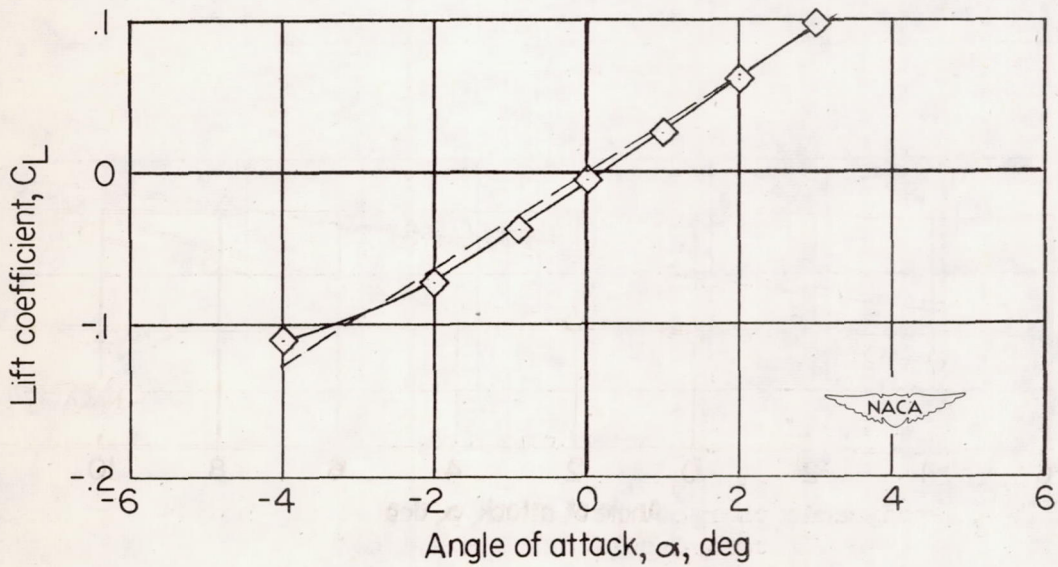
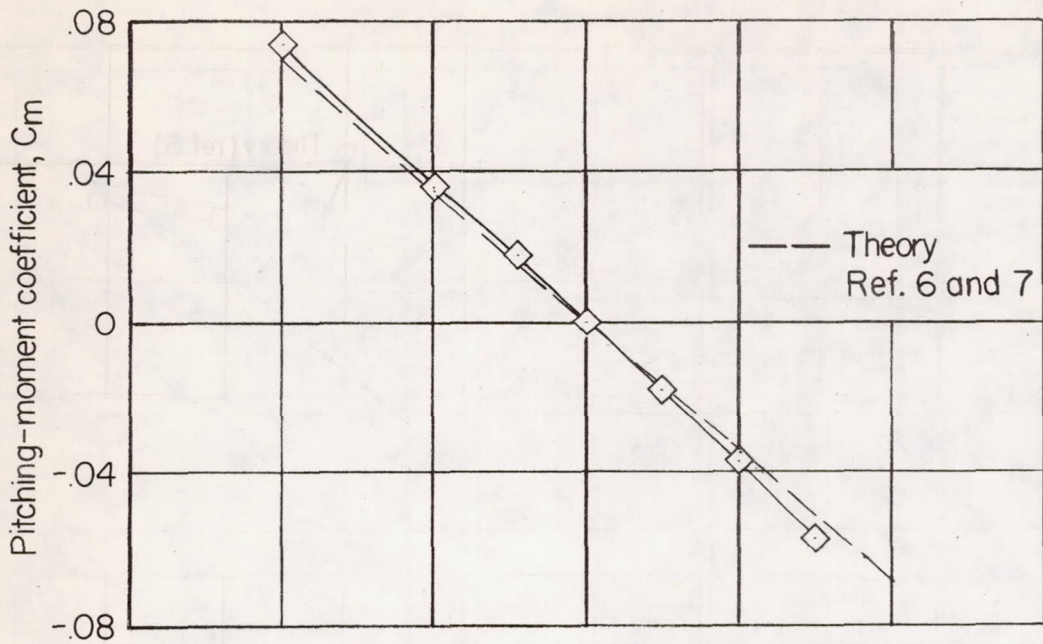


Figure 15.- Aerodynamic characteristics in pitch of the body + wing.
 $M = 1.61$.

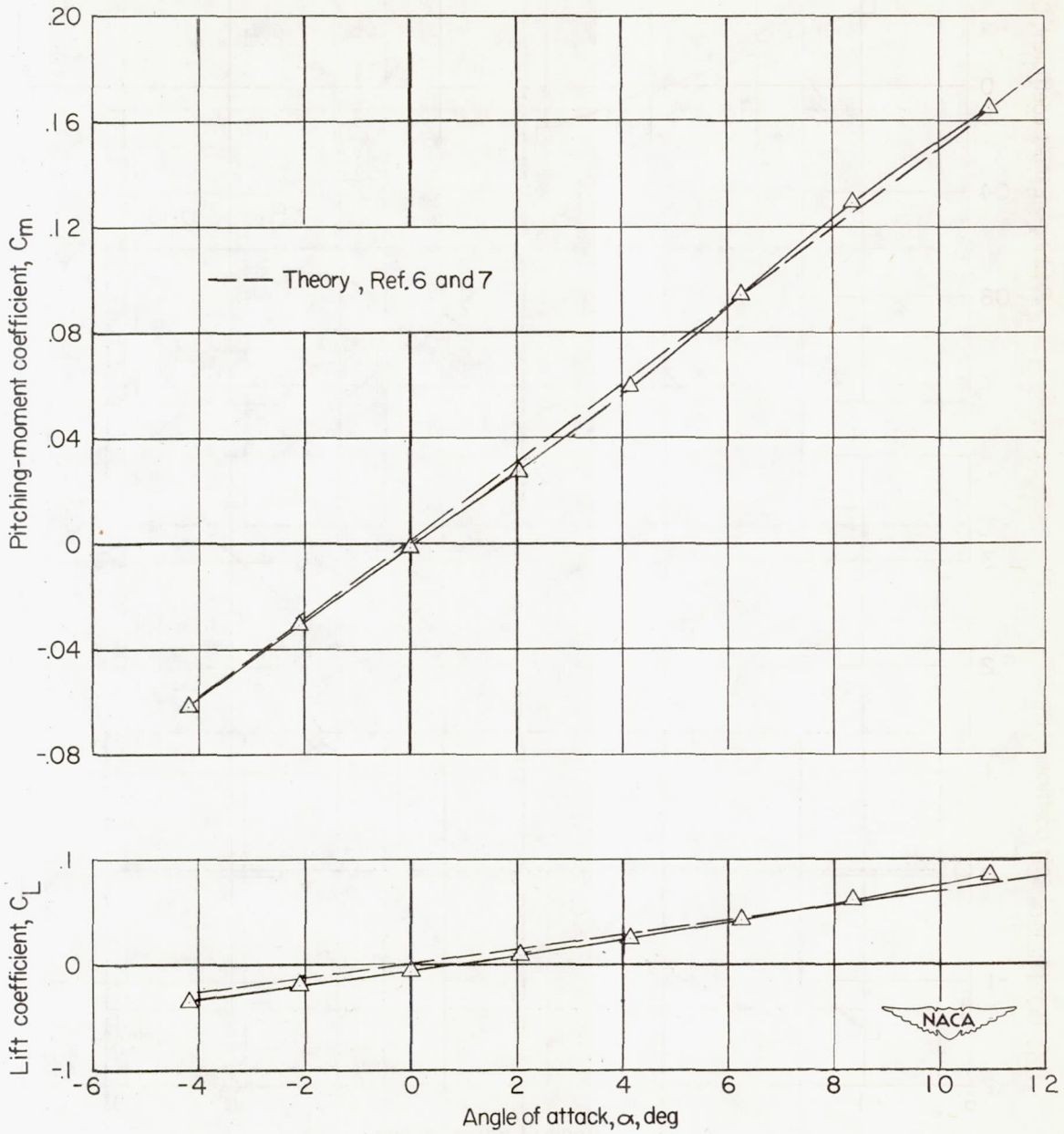


Figure 16.- Aerodynamic characteristics in pitch of the body + horizontal canard surfaces. $M = 1.61$.

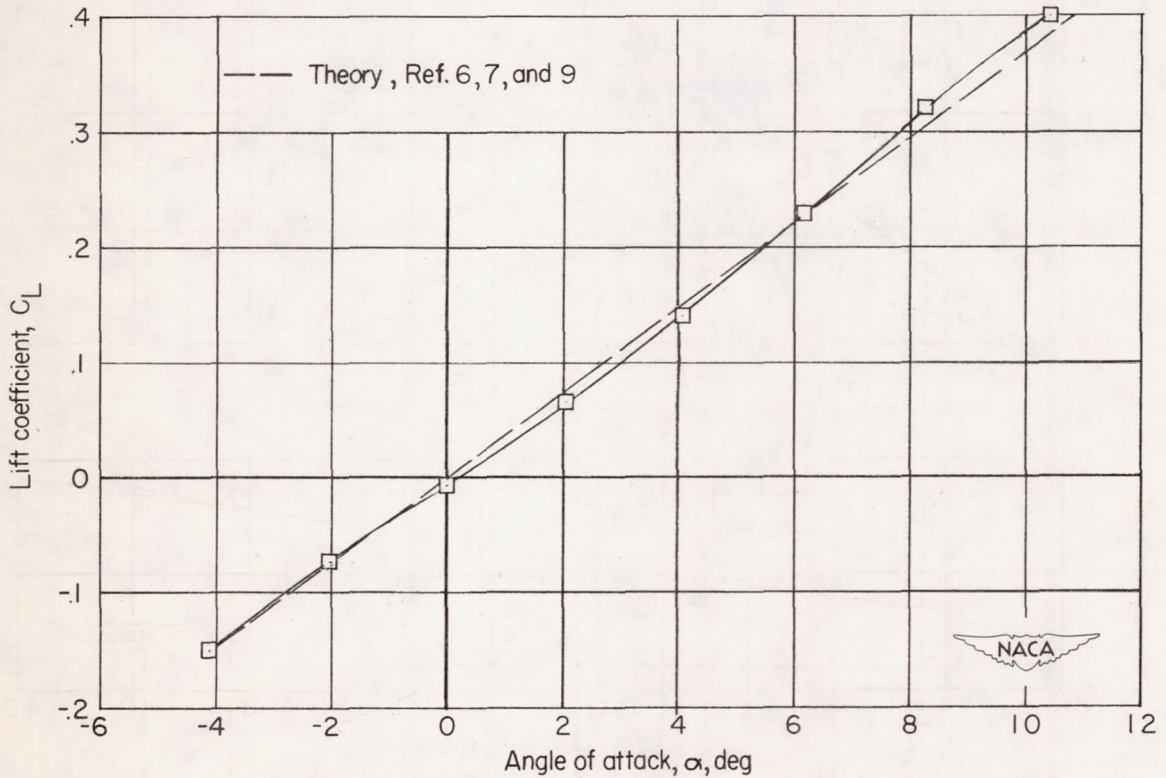
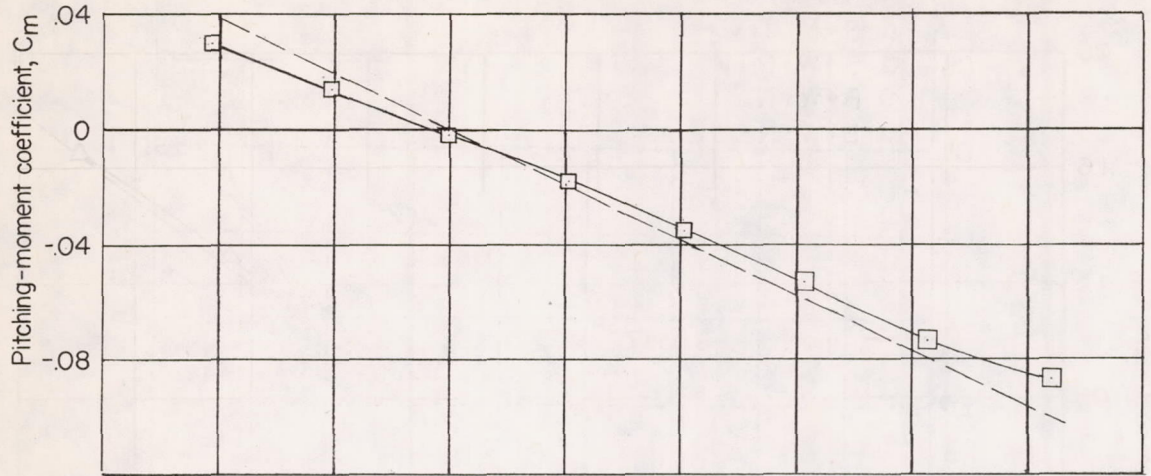
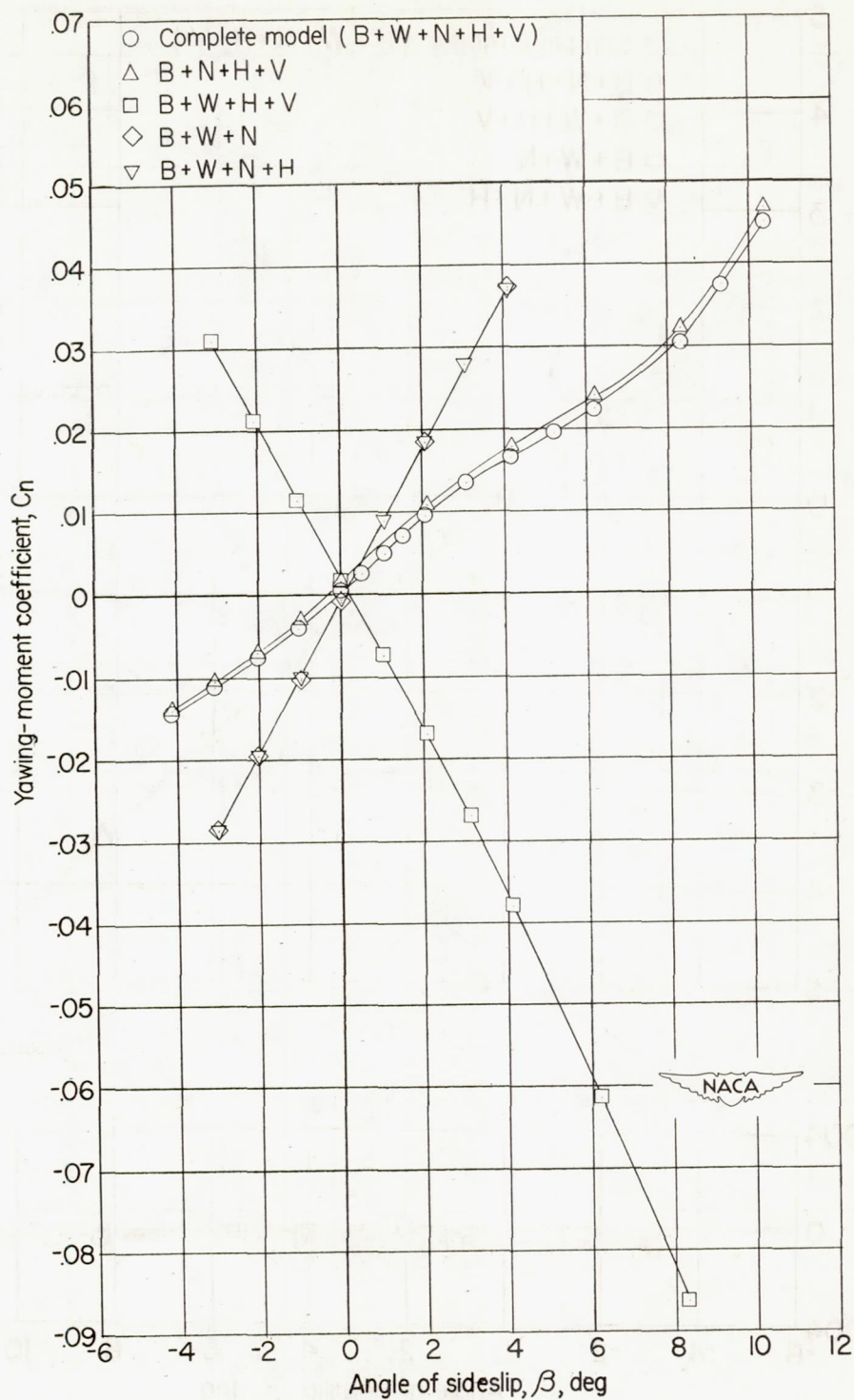
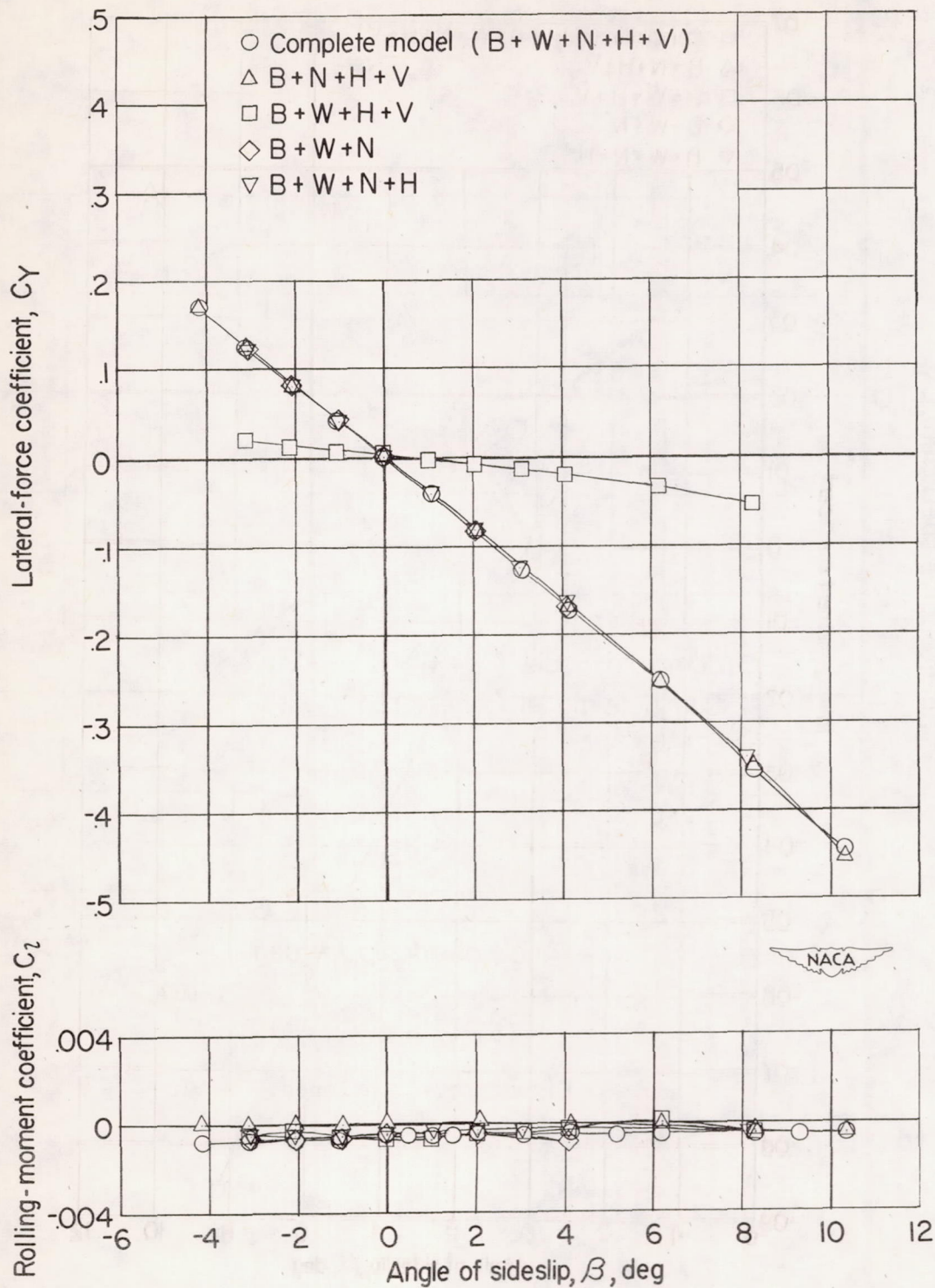


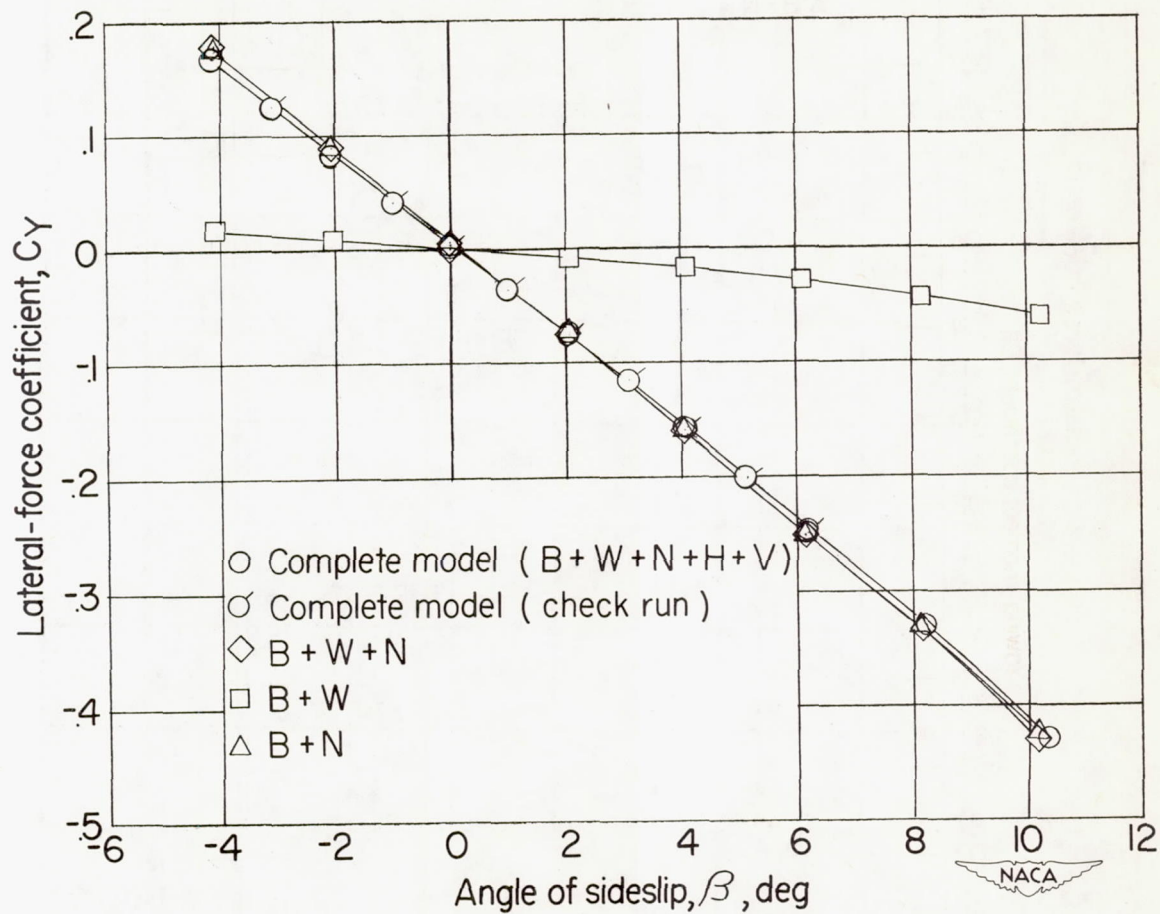
Figure 17.- Aerodynamic characteristics in pitch of the body + wing + horizontal canard surfaces. $M = 1.61$.

(a) $\alpha = 0^\circ$.Figure 18.- Effect of various components on the aerodynamic characteristics in sideslip of the complete basic model. $M = 1.61$.



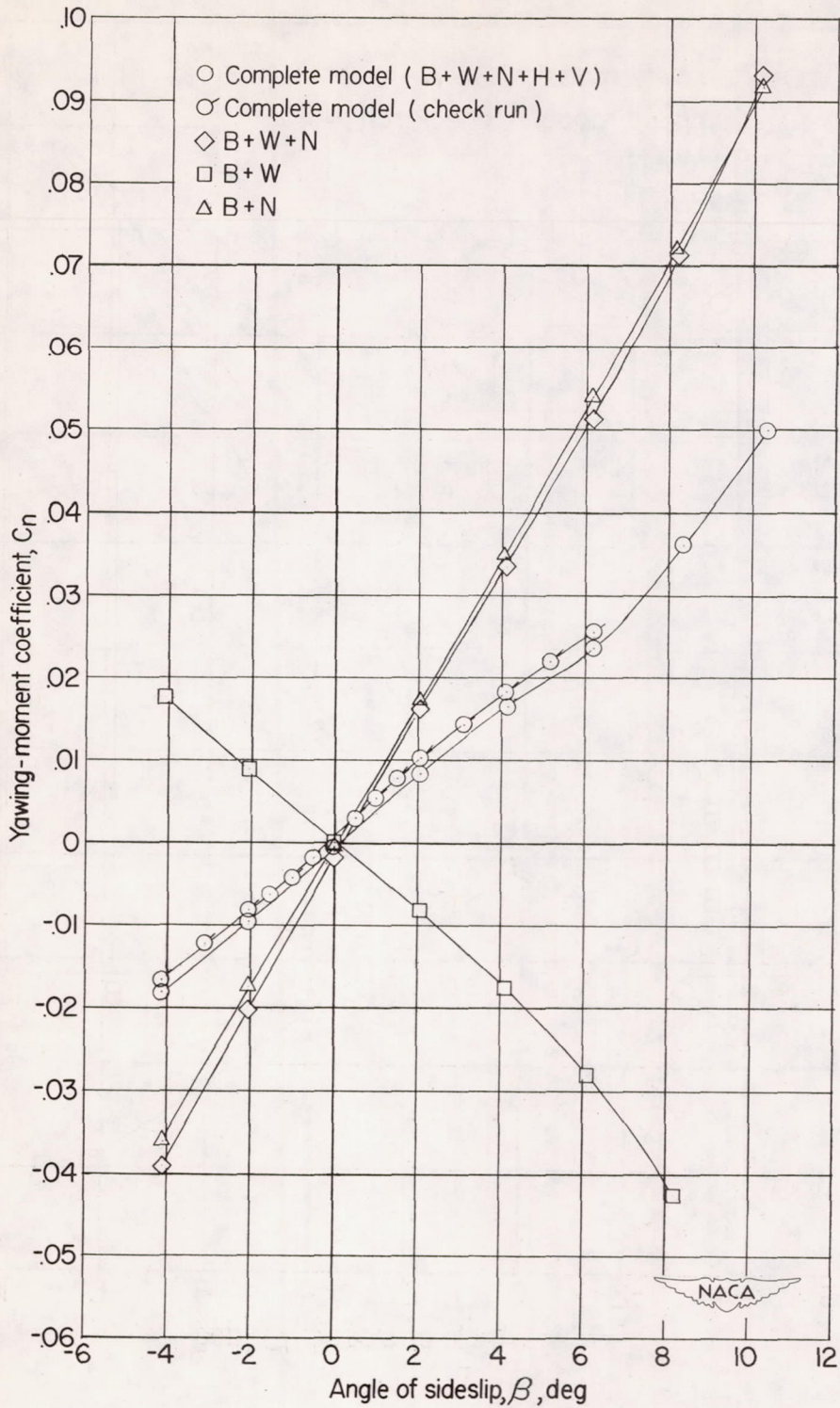
(a) Concluded.

Figure 18.- Continued.



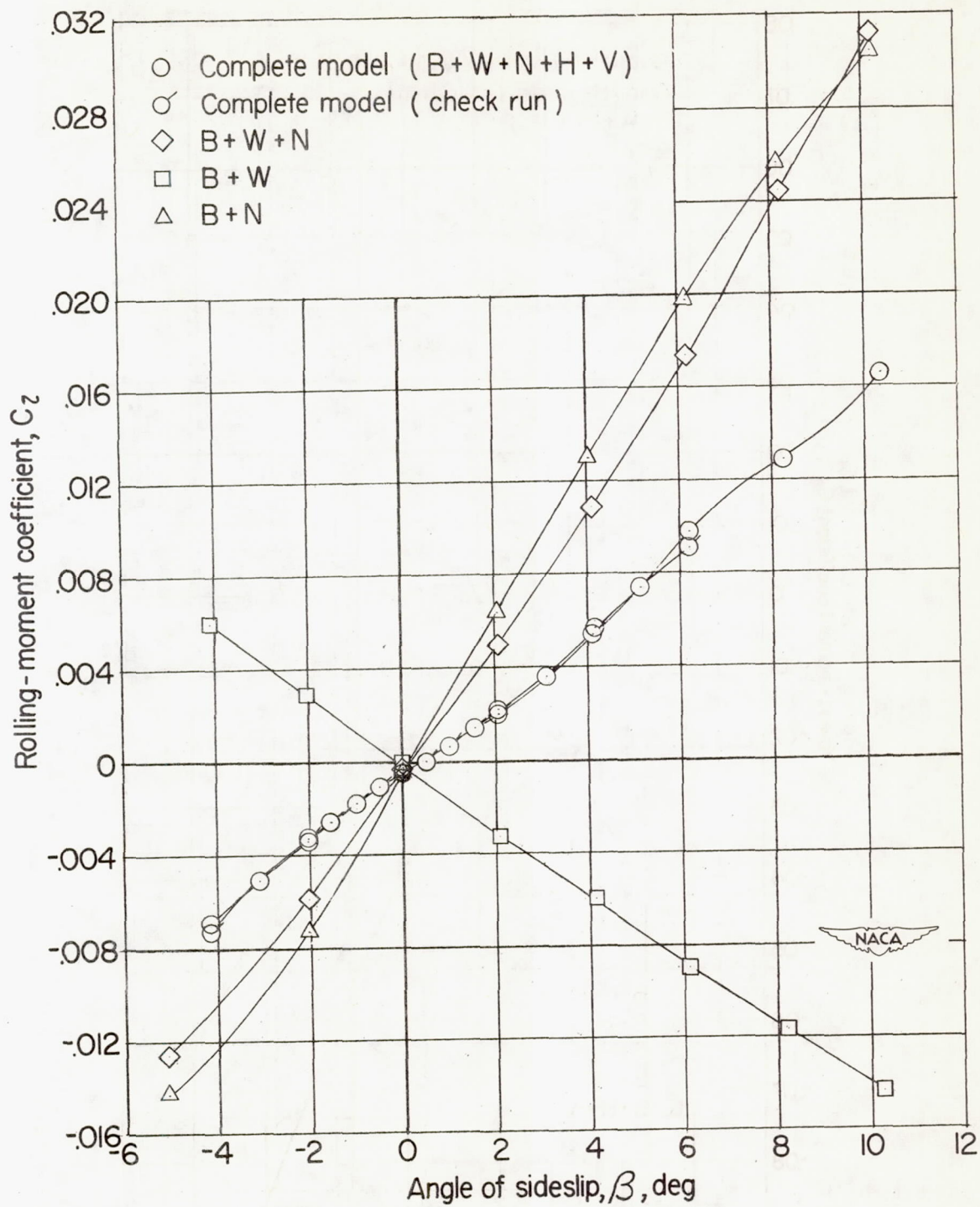
(b) $\alpha = 6.3^\circ$.

Figure 18.- Continued.



(b) Continued.

Figure 18.- Continued.



(b) Concluded.

Figure 18.- Concluded.

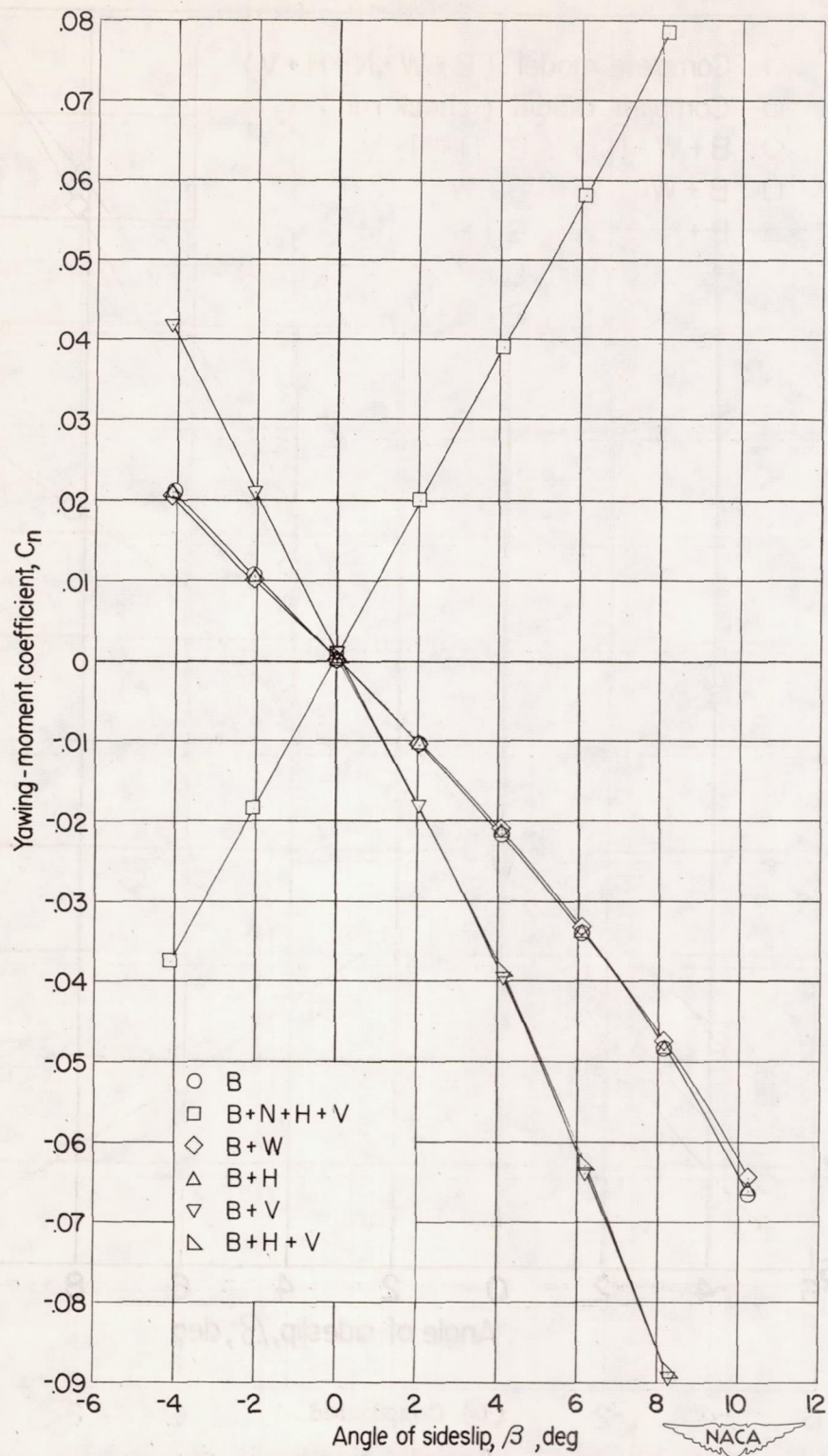


Figure 19.- Effect of the various components on the aerodynamic characteristics in sideslip of the body alone. $\alpha = 0^\circ$, $M = 1.61$.

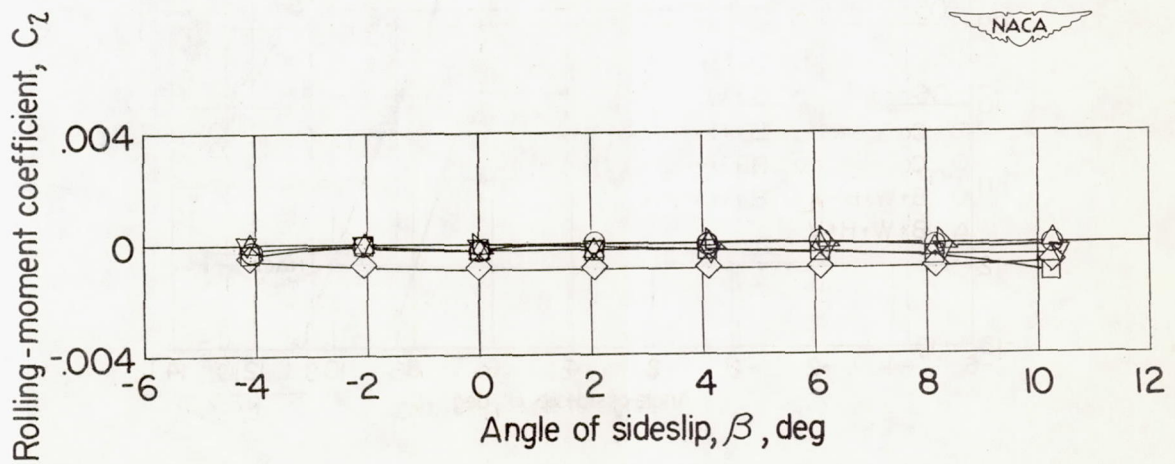
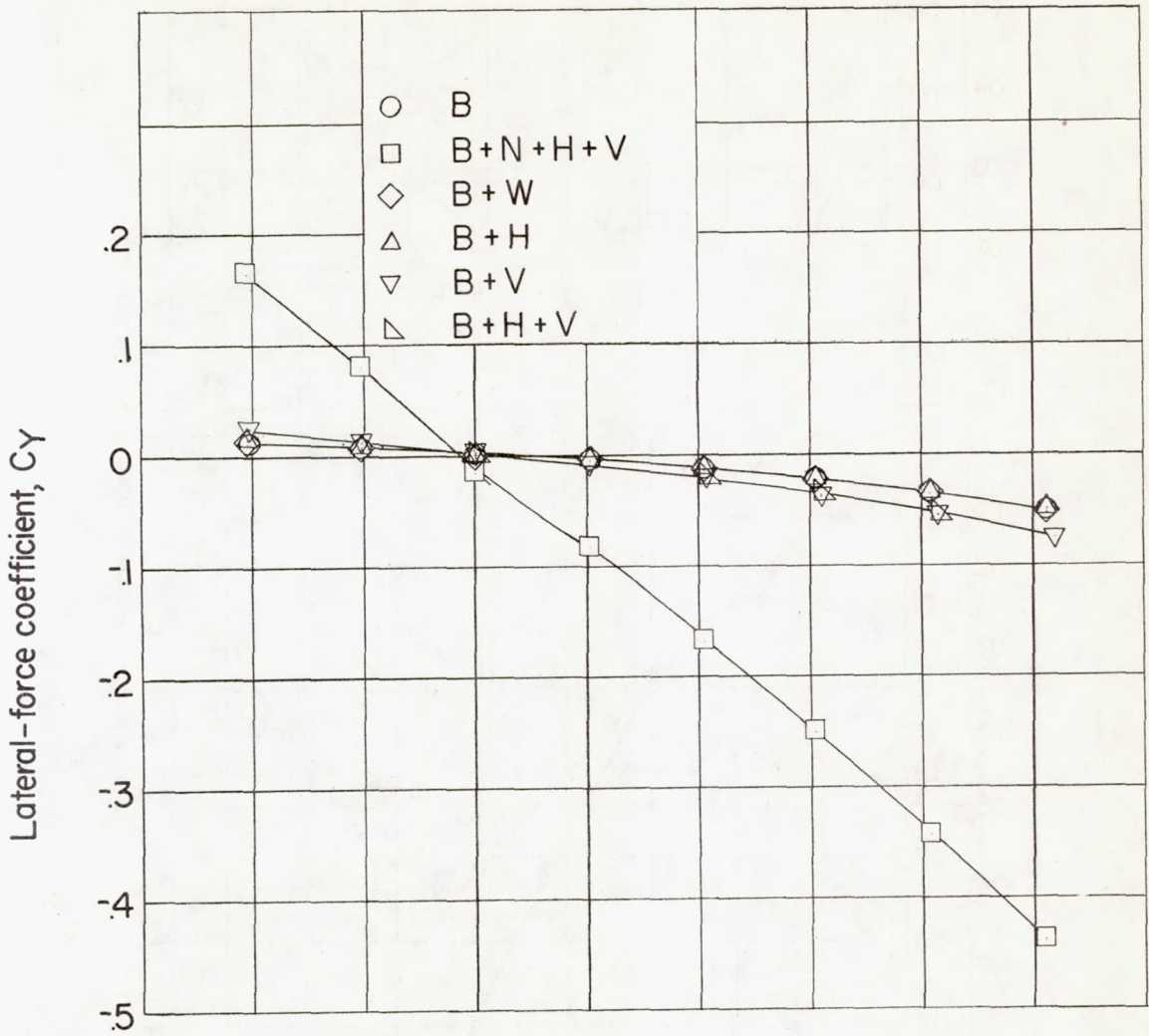


Figure 19.- Concluded.

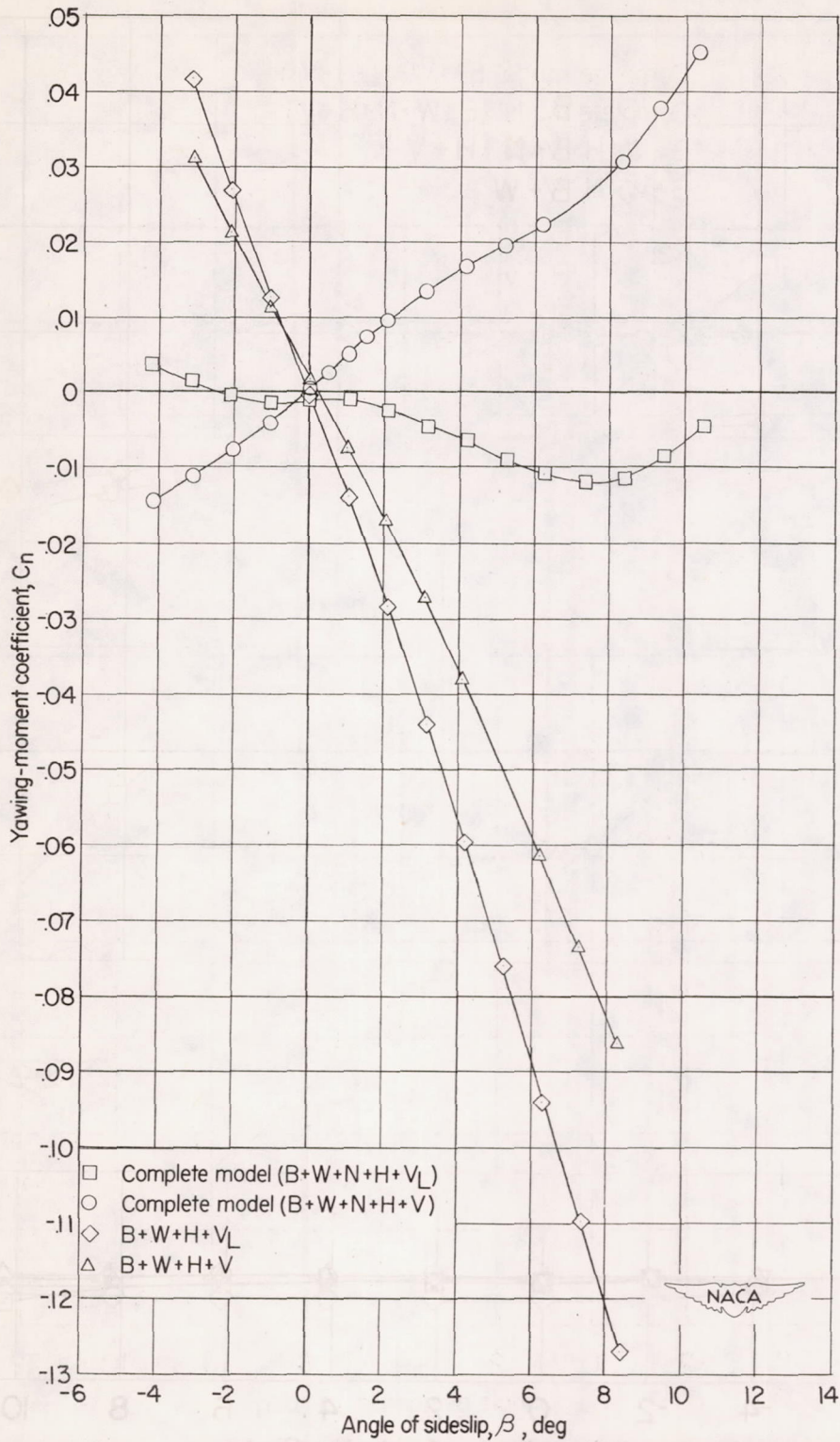


Figure 20.- Effect of vertical canard size on the aerodynamic characteristics in sideslip of the complete basic model. $\alpha = 0^\circ$, $M = 1.61$.

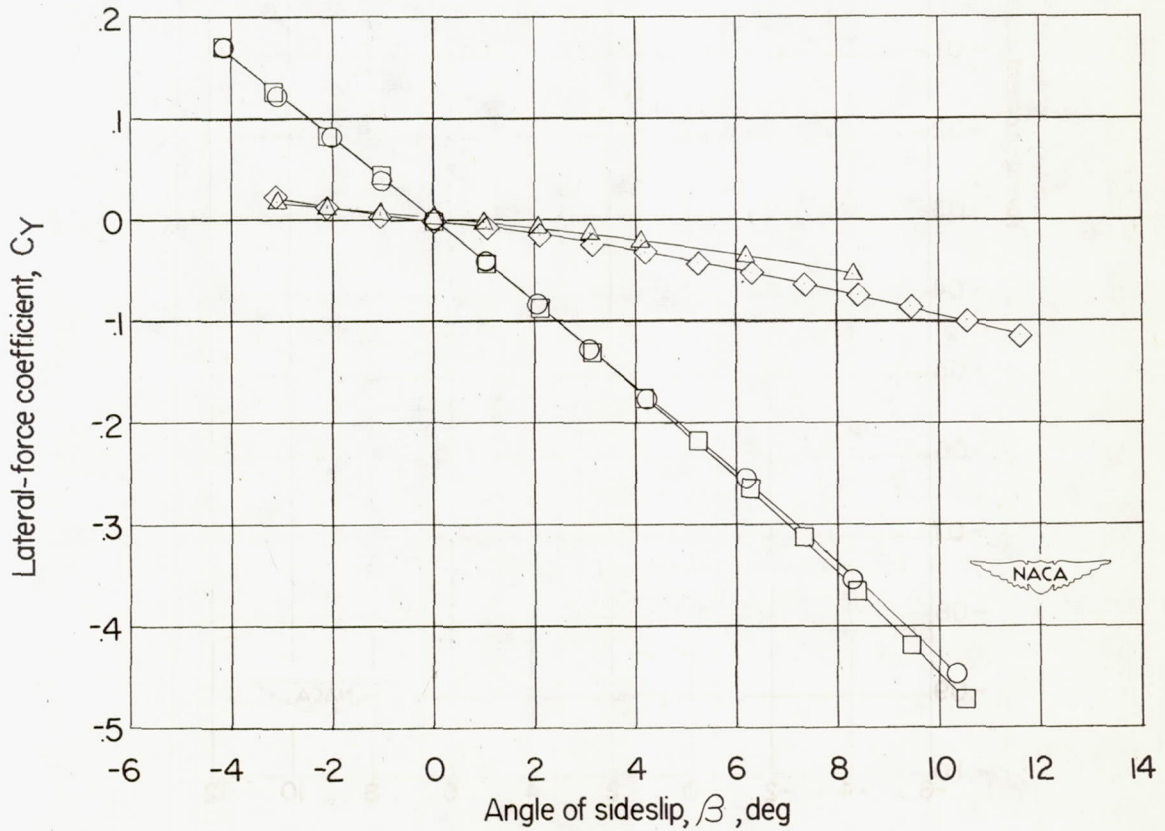
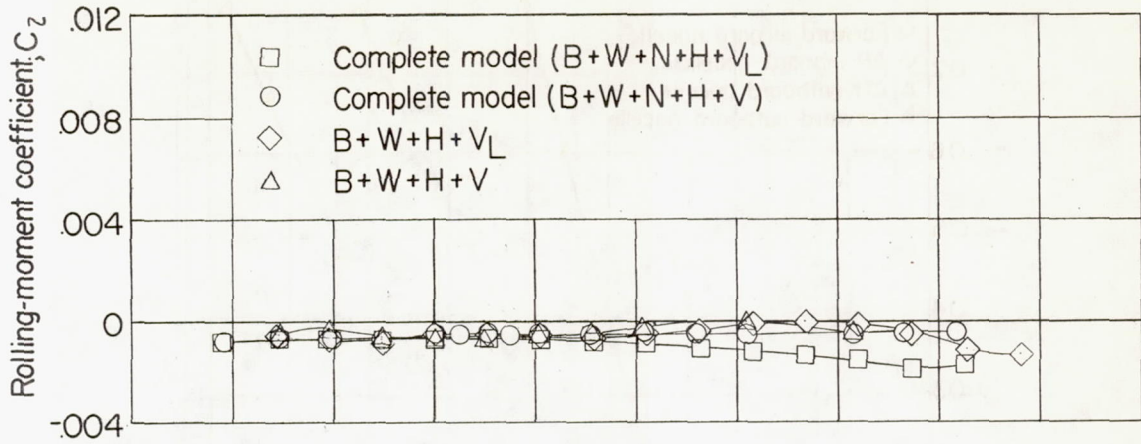


Figure 20.- Concluded.

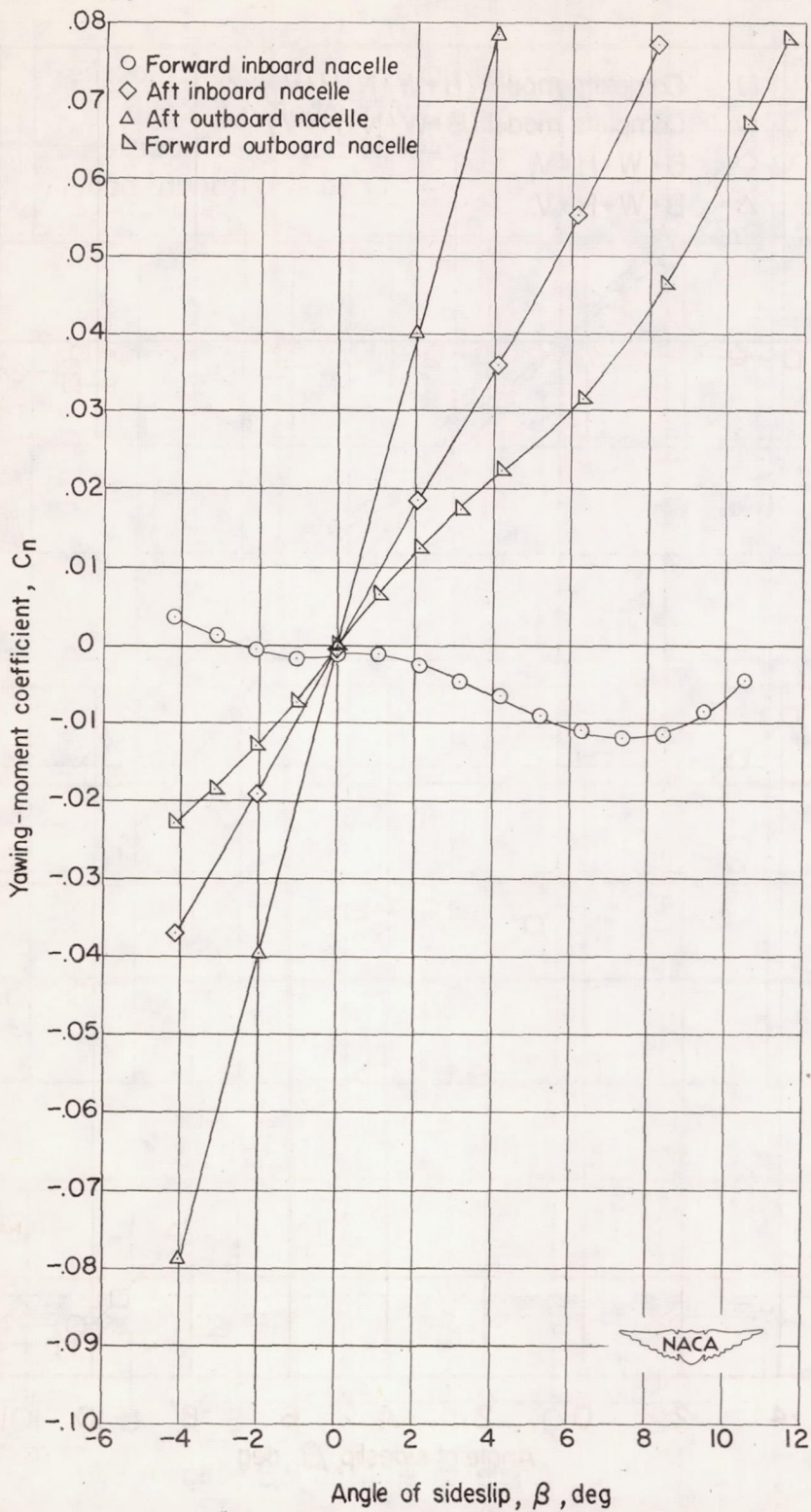


Figure 21.- Effect of nacelle position on the aerodynamic characteristics in sideslip of the complete model. $M = 1.61$.

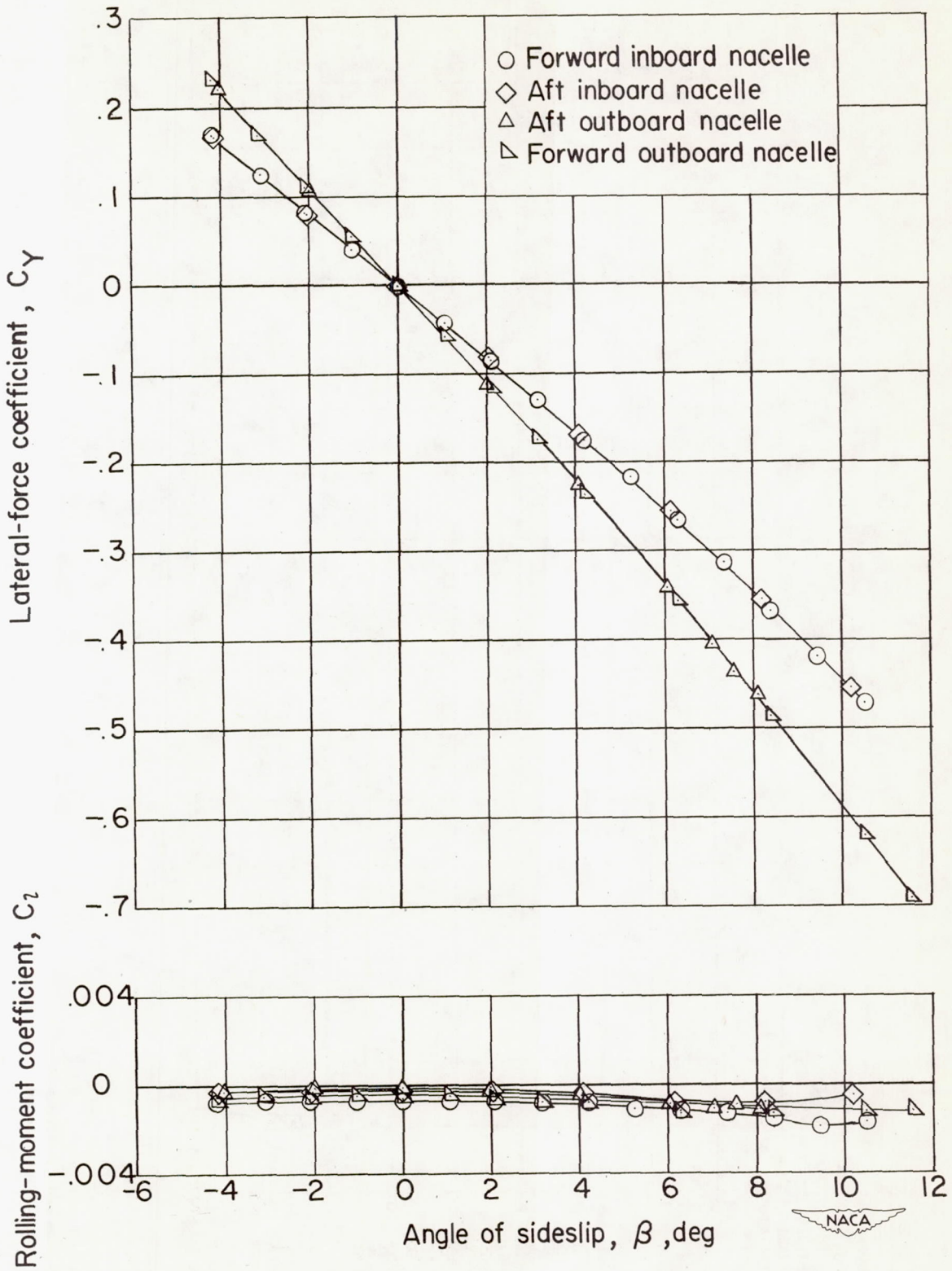


Figure 21.- Concluded.